On the harmonic analysis of cup anemometer rotation speed: A principle to monitor performance and maintenance status of rotating meteorological sensors

Santiago Pindado *, Javier Cubas, Félix Sorribes-Palmer

Instituto Universitario de Microgravedad "Ignacio Da Riva" (IDR/UPM), Universidad Politécnica de Madrid, ETSI Aeronáuticos

A B S T R A C T

The calibration results of one anemometer equipped with several rotors, varying their size, were analyzed. In each case, the 30-pulses pert turn output signal of the anemometer was studied using Fourier series decomposition and correlated with the anemometer factor (i.e., the anemometer transfer function). Also, a 3-cup analytical model was correlated to the data resulting from the wind tunnel measurements. Results indicate good correlation between the post-processed output signal and the working condition of the cup anemometer. This correlation was also reflected in the results from the proposed analytical model. With the present work the possibility of remotely checking cup anemometer status, indicating the presence of anomalies and, therefore, a decrease on the wind sensor reliability is revealed.

1. Introduction

Today, the use of wind speed anemometers is very common, their applications having spread from sectors such as meteorology or wind energy to others where the effect of the wind can be important (moving bridges in civil engineering, big cranes, etc.). Nevertheless, the wind energy industry still can be considered as the biggest consumer of anemometers all over the world. Apart from the fact that the wind power is proportional to the third power of the wind speed, which underlines the importance of having the most accurate instruments [1], the wind energy sector is extremely concerned with two aspects that, despite technological advances such as LIDAR and SODAR [2–5], require the use of anemometers: wind energy production forecast on the field, and wind turbine performance control [6]. Within the past decades the wind energy sector has been openly supported by governments (Germany, Denmark, Spain...), concerned about clean energies and a reduction of their dependence on fossil fuels [7]. In addition, new strong players in this industry like China, U.S.A., Brazil or India are now being very active, with high figures in terms of installed wind power and growing rates.[1] According to these facts it seems reasonable to assume that the mentioned massive demand of anemometers from this sector will be maintained in the incoming years, if not increased. Among the different instruments devoted to measure the wind speed, the cup anemometer remains today the most used in the wind energy sector [8], as it is inexpensive when compared to other devices (e.g., sonic anemometers), shows linear response in the normal wind speed range (from 4 m s^{-1} to 16 m s^{-1}) [9], and is capable to operate in quite extreme weather conditions [10].

[1] Global Wind Energy Council; US Energy Information Administration.

The present paper is part of the IDR/UPM Institute's research framework on cup anemometer performance, which includes a review of large series of calibrations performed on commercial anemometers [8], the analysis of aging and the climatic effects on anemometer transfer function [11,12], the experimental study of the cups and rotor shapes on anemometer response [13–15], and the review and improvement of analytical methods to study anemometer performance in order to have a better understanding of the physics regarding its rotation (aerodynamics, friction, etc.) [8,13–16].

1.1. Modeling the cup anemometer performance in steady conditions

From the wind industry point of view, the cup anemometer performance is based on the transfer function:

$$V = A \cdot f + B, \tag{1}$$

where V is the wind speed, f is the anemometer's rotation frequency output, and A (slope) and B (offset) are the calibration coefficients. This linear equation,[2] defined in the first quarter of the 20th century for the Robinson-type anemometer[3] [17], correlates the wind speed and the anemometer's output frequency [18], and must be defined by means of a calibration process [19–22]. In order to have an expression with a clearer physical meaning, the transfer function can be rewritten in terms of the anemometer's rotation frequency, f_r, instead of the output frequency, f, introducing in the expression the number of pulses per revolution given by the anemometer, N_p:

$$V = A \cdot N_p \cdot f_r + B = A_r \cdot f_r + B. \tag{2}$$

The above equation also allows a direct comparison between different anemometers [8], and between analytical models and experimental results [23,24]. The number of pulses, N_p, is different depending on the anemometer's inner system for translating the rotation into electric pulses. Magnet-based systems give 1–3 pulses per revolution, whereas optoelectronics-based systems normally give higher pulse rates per revolution, from 6 to 44 [8].

To analyze the behavior of cup anemometer, analytical models have been proposed by other authors in the past. These models are developed from the following expression [19]:

$$I\frac{d\omega}{dt} = Q_A + Q_f, \tag{3}$$

where I is the moment of inertia of the rotor, Q_A is the aerodynamic torque, and Q_f is the frictional torque that depends on the air temperature, T, and the rotation speed, ω (from [25]: $Q_f = B_0(T) + B_1(T)\omega + B_2(T)\omega^2$, where coefficients B_0, B_1, and B_2 are negative[4]). The frictional torque, Q_f, can be neglected as it is normally very small in comparison to the aerodynamic torque [26,27]. The aerodynamic torque, Q_A, can be derived from the aerodynamic forces on the rotor cups, which are normally measured in a wind tunnel in "static" configuration, that is, measuring the forces on an isolated and fixed cup immersed in a constant wind speed air flow and without considering any rotational speed [13,14,28]. The aerodynamic torque due to one single cup is expressed as a function of the aerodynamic normal-to-the-cup force coefficient measured in a wind tunnel, c_N, the wind speed, V, the rotation speed, ω, the cup radius, R_c, the cup center rotation radius, R_{rc}, and the air density, ρ. See in Fig. 1 the normal-to-the-cup force coefficient, c_N, measured on hemispherical and conical cups in "static" configuration, as a function of the wind angle with respect to the cup, α, [28].

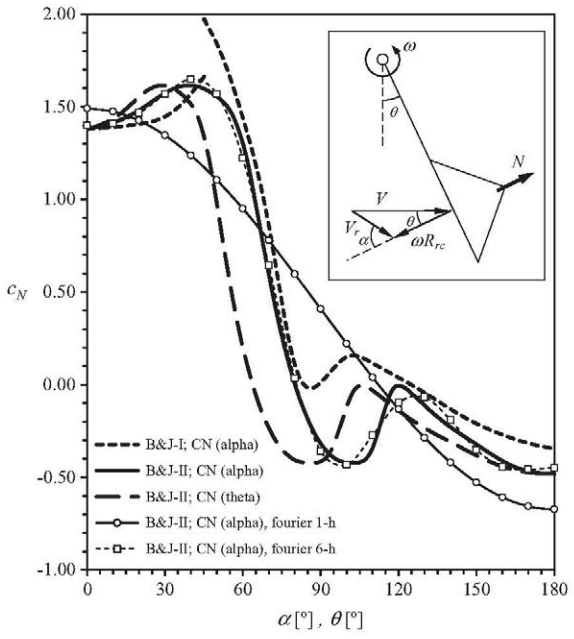

Fig. 1. Normal aerodynamic force coefficient, c_N, of the Brevoort & Joyner Type-I (hemispherical) and Type-II (conical) cups [28], plotted as a function of the wind direction with respect to the cup, α. The coefficient regarding Type II cup is also plotted as a function of the rotor's rotation angle, θ (calculated with expression (6) for an anemometer factor $K = 3.5$). See in the sketch the variables involved in the rotation of an anemometer cup: normal aerodynamic force on the cup, N, wind speed, V, relative wind speed to the cup, V_r, rotor rotation angle, θ, rotor rotational speed, ω, and wind direction with respect to the cup, α. The 1-harmonic term Fourier series approximation (expression (9)) to the Type-II cup has been plotted, together with the 6-harmonic terms Fourier series approximation [14].

As far as the authors' knowledge goes, the first analytical model was developed by Schrenk [29] in 1929. This 2-cup positions model relates the aforementioned aerodynamic torque, Q_A, to the rotation speed, ω, the wind speed,

[2] Some authors claim that a non-linear expression should be used instead of a linear one, especially at low wind speeds [10].

[3] The cup anemometer invented by Robinson in the XIX century [66–68] had four cups/arms instead of three, which is the present standardized configuration thanks to the work of Patterson [31], who found that the "3-cup anemometer is decidedly superior to the 4-cup" due to a quicker and more uniform response, and a higher aerodynamic torque produced by the cups [69–71]. In 1924 the 3-cup anemometer was adopted as a standard for meteorology in the United States of America and Canada [69].

[4] The friction torque, Q_f, in expression (3) has a negative sign in the updated version of reference [19]. Therefore, coefficients B_0, B_1 and B_2 of the friction torque expression will be positive, if this is taken into account.

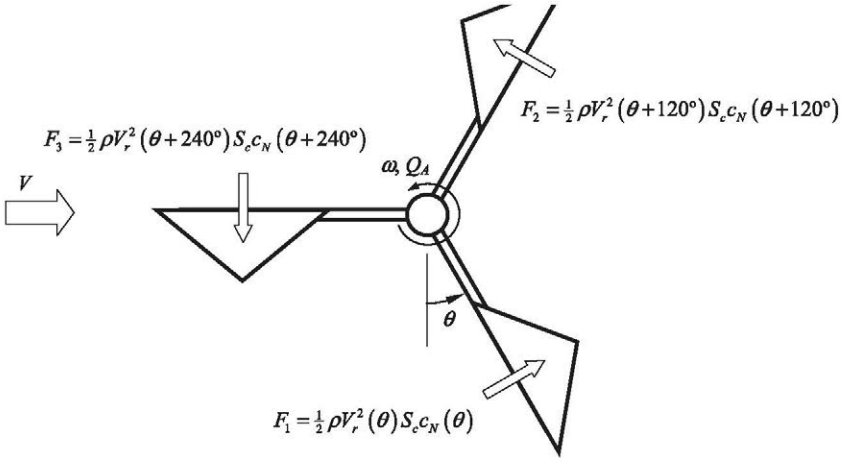

Fig. 2. Sketch of the 3-cup analytical model configuration.

V, and the aerodynamic normal coefficient, c_N, measured at two wind speed angles, that is, at two positions of the cups, $\alpha = 0°$ ($c_{D1} = |c_N(0)|$ in Fig. 1) and $\alpha = 180°$ ($c_{D2} = |c_N(180)|$ in Fig. 1). This model has been widely used to study the cup anemometer performance [16,30]. Although this 2-cup analytical model has correlated well to experimental calibration results from different commercial anemometers [8], it is fair to say that it has certain limitations, derived from the fact that the behavior of the rotor is based on two positions of the cups only.

To have a better approach to the problem, the 3-cup analytical model was developed integrating the aerodynamic normal force on all three cups in an entire rotation [13,23,24]. The starting point of this 3-cup model is the mentioned expression (3), taking into account, as said, the aerodynamic torque produced by each cup of the anemometer rotor, see Fig. 2. If friction is also left out of Eq. (3), the following expression can be derived then for the rotor movement:

$$I\frac{d\omega}{dt} = \frac{1}{2}\rho S_c R_{rc} V_r^2(\theta) c_N(\alpha(\theta)) + \frac{1}{2}\rho S_c R_{rc} V_r^2(\theta + 120°) c_N(\alpha(\theta + 120°)) + \frac{1}{2}\rho S_c R_{rc} V_r^2(\theta + 240°) c_N(\alpha(\theta + 240°)), \quad (4)$$

where V_r is the wind speed relative to the cups, c_N is the aerodynamic normal force coefficient, α is the local wind direction with respect to the cups, θ is the angle of the rotor with respect to a reference line (see sketch in Fig. 1), and S_c is the front area of the cups ($S_c = \pi R_c^2$). Wind speed V_r, relative to the cup at rotor angle θ with respect to the reference line, is expressed as:

$$V_r(\theta) = \sqrt{V^2 + (\omega R_{rc})^2 - 2V\omega R_{rc}\cos(\theta)}, \quad (5)$$

whereas the wind direction with respect to the cup, α, can be derived, as a function of the rotor's position angle, θ, from the following expression [13]:

$$\tan(\alpha) = \frac{K\sin(\theta)}{K\cos(\theta) - 1}, \quad (6)$$

where K is the anemometer factor, defined as the ratio between the wind speed, V, and the speed of the cup center averaged in one complete rotation, ωR_{rc} [9,31]:

$$K = \frac{V}{\omega R_{rc}} = \frac{A_r f_r + B}{2\pi f_r R_{rc}} = \frac{A_r}{2\pi R_{rc}} \frac{1}{1 - \left(\frac{B}{V}\right)}. \quad (7)$$

In the present work the anemometer factor is considered leaving aside the offset of the transfer function, B, as it is normally very small when compared to the wind speed:[5]

$$K = \frac{A_r}{2\pi R_{rc}}. \quad (8)$$

1.1.1. Modeling the aerodynamic forces on the cups

The aerodynamic normal force coefficient, c_N, can be simplified taking into account only the two first coefficients of the Fourier series expansion [14]:

$$c_N(\alpha) = c_0 + c_1\cos(\alpha). \quad (9)$$

Also, the related-to-the-cup wind angle, α, was quite accurately related to the rotor's rotation angle, θ, with the expression:

$$\cos(\alpha) = \eta_0 + \eta_1\cos(\theta) + \eta_2\cos(\theta)^2 + \eta_3\cos(\theta)^3, \quad (10)$$

where the coefficients η_0, η_1, η_2, and η_3 are expressed as a function of anemometer factor K:

$$\eta_0 = \frac{-1}{\sqrt{1+K^2}}; \quad \eta_1 = \frac{K}{\sqrt{1+K^2}} - \frac{1}{K^2-1};$$
$$\eta_2 = \frac{1}{\sqrt{1+K^2}}; \quad \eta_3 = \frac{K^2}{K^2-1} - \frac{K}{\sqrt{1+K^2}}. \quad (11)$$

Taking into account expressions (9) and (10), Eq. (4) can be solved for the stationary state, averaging its value along one turn of the rotor. Then, a direct relationship between the anemometer factor and coefficients c_0 and c_1 is derived:

[5] The offset wind speed, B, of the transfer functions related to most of Class 1 anemometers is normally lower than 0.25 m s^{-1} and negligible [8]. However, the effect of this constant should be taken into account for calculations at low wind speeds [15].

$$0 = \left(1 + \frac{1}{K^2}\right)\left(c_0 + c_1\left(\eta_0 + \frac{1}{2}\eta_2\right)\right) - \frac{c_1}{K}\left(\eta_1 + \frac{3}{4}\eta_3\right). \tag{12}$$

Using expressions (11), the above equation was finally rewritten in terms of the anemometer factor:

$$0 = \left(1 + \frac{1}{K^2}\right)\left(1 - \frac{1}{2}\frac{c_1}{c_0}\frac{1}{\sqrt{1+K^2}}\right) - \frac{1}{4}\frac{c_1}{c_0}\frac{1}{K}\left(\frac{K}{\sqrt{1+K^2}} + \frac{3K^2-4}{K^2-1}\right). \tag{13}$$

This equation gives, as a function of the Fourier coefficients ratio c_1/c_0 (that only depends on the aerodynamics of the cup), the anemometer factor, K, and then, for each wind speed, V, the averaged value of the rotational speed of the rotor, ω, can be obtained from expression (7). This 3-cup model has been successfully correlated with experimental results [14].

1.1.2. Modeling the rotor's response

Additionally, if the attention is focused on the left term of Eq. (4), we should bear in mind that this term is not equal to zero, although its average value is. Under a perfectly constant, horizontal and uniform wind speed, and considering the stationary condition, the rotational speed corresponding to a 3-cup rotor can be decomposed along one turn into a constant term, ω_0, plus one harmonic term that corresponds to a frequency three times bigger than the one related to the mentioned constant term, $3\omega_0$, and its multiples, $6\omega_0$, $9\omega_0$, $12\omega_0$...[15]:

$$\omega(t) = \omega_0 + \sum_{n=1}^{\infty} \omega_{3n} \sin(3n\omega_0 t + \varphi_{3n}). \tag{14}$$

Obviously, for a cup anemometer in a real situation, that is, taking into account some degree of turbulence, wind non-uniformities, the wake created downstream the anemometer's body, etc., other harmonic terms not multiple of 3 should be included in the above equation as a result of the Fourier expansion:

$$\begin{aligned}\omega(t) &= \omega_0 + \omega_1 \sin(\omega_0 t + \varphi_1) + \omega_2 \sin(2\omega_0 t + \varphi_2) \\ &\quad + \omega_3 \sin(3\omega_0 t + \varphi_3) \ldots \\ &= \omega_0 + \sum_{n=1}^{\infty} \omega_n \sin(n\omega_0 t + \varphi_n).\end{aligned} \tag{15}$$

Nevertheless, taking into account results measured on damaged anemometers [32], expression (15) can be quite accurately simplified by taking only the constant term, ω_0, and the first and third harmonic terms of the series:

$$\omega(t) = \omega_0 + \omega_1 \sin(\omega_0 t + \varphi_1) + \omega_3 \sin(3\omega_0 t + \varphi_3), \tag{16}$$

as the third harmonic term is the most important due to the cup anemometer shape (which produces three accelerations and three decelerations of the rotor in one turn), while the first harmonic reflects the anomalies that affect the normal rotation of the anemometer's rotor.

1.2. Understanding of the rotational speed harmonic terms

The aim of the present work is to have a better understanding of the effect of the first and the third harmonic terms, ω_1 and ω_3, on cup anemometer performance, continuing the experimental research already initiated in [15]. The analytical relationship between this third harmonic term and the coefficients c_0 and c_1 (from the simplified expression of the aerodynamic normal force coefficient, c_N, see Eq. (9)), is also analyzed for both stationary and transient cases. Besides, the first harmonic term is studied as a way to analyze the evolution of cup anemometer performance degradation. The idea behind this research is the attempt to establish some parameter related to the anemometer wear and tear in order to optimize the maintenance processes, as around 30% of mast-mounted anemometers return for recalibration far from normal operational conditions [33]. Some effort has been done to monitor the status of anemometers, as their working condition when operating in the field must be checked through frequent calibrations [34]. Calibration-on-the-field procedures have been studied as a cost-effective solution in order to reduce anemometer maintenance and recalibration [35,36]. This problem is a major concern in the industry, and as a result several patents and inventions have been developed. The procedure behind some of them is based on forcing the anemometer's rotation and then correlating its response with the corresponding input [37–41], whereas other patents are based on the correlation between the measured wind speed by the anemometer and a different parameter related to the wind speed, e.g., the power curve of a wind turbine [42–45].

Anomaly detection is quite an important problem within many industrial, technological and research areas, with three classical approaches [46]:

- Case-based reasoning, based on a list of rules derived from wide human experience.
- Model-based diagnosis, in which the decision criteria are based on mathematical models associated to physical attributes. Some parameters with physical meaning are then monitored as indicators of the possible degradation of the system.
- Non-parametric models such us neural network-based methods. This approach does not require expert knowledge. However, a huge amount of training data needs to be post-processed in order to validate the model.

The present work should be considered then an effort to identify a new parameter, the first harmonic term of the rotation speed, to be used in anemometer condition diagnosis. Focusing on the cup anemometer as a mechanism, it is logical to assume that any malfunction of the anemometer bearings system, or any defect produced on the rotor geometry (dirt accumulation, broken parts...), should be translated into noise added to the output signal. Apart from the fact that this noise means a change of the transfer function constants and, consequently, a degradation of anemometer performance (lower rotation frequency at same wind velocity), it can be assumed that it is formed by a number of signal perturbations that are

repeated each turn of the rotor. So, in principle, any degradation or change of the anemometer's working condition should be translated into an increase of the first harmonic term of Eq. (15). This kind of analysis based on the harmonic response has been traditionally used for wind turbine condition monitoring. These machines, that involve several rotating systems (gear, bearings, shaft), include different sensors and transducers (position, velocity, and acceleration) used to monitor the maintenance status through Fourier analysis of vibrations spectra [47–50].

In addition, it should be pointed out that fault detection in mechanical units such us cup anemometers is usually carried out by performance monitoring, this process requiring large time-series processing [51]. Different techniques have been developed to reduce the complexity of working with that large time-series. The normal way to perform this reduction is to characterize the time-series by a spectral decomposition (other characterizations as wavelet decomposition or singular value decomposition are also possible) [52–54]. The harmonic terms of the cup anemometer rotation speed defined in the present work can be considered equivalent to the spectral decomposition.

In this context, the PHM 2011 Data Challenge Competition should be mentioned, as it was a very interesting proposal to analyze the problem of cup anemometer status based on the measurements record. In this competition, a set of measurements (mean, standard deviation, maximum and minimum wind speed), taken by several paired anemometers installed at different heights along a vertical mast were analyzed in order to study the anemometers' working condition. Different solutions were obtained by researchers who took part in the aforementioned competition, the most relevant being based on direct comparison of signals from two different cup anemometers once properly filtered [55], the correlation of the differences in measured wind speed from two anemometers with a Weibull distribution [56], and the use of a neural network model [57]. The last approach, i.e., the use of neural network models, seems to be a quite accurate tool for cup anemometer performance analysis, as it obtained the highest score in the PHM 2011 Data Challenge Competition, and it has also been used with good results to compensate anemometer overspeeding in real-time measurements [58].

This work is organized as follows. In Section 2 the testing methodology and results post-processing carried out in the present research are described. The results are discussed in Section 3, which is divided in three subsections. The first subsection is devoted to a first analysis of the testing results, whereas the second and the third subsections include the development of an analytical methodology based on harmonic decomposition, to study respectively the cup anemometer working under optimal conditions and under the effect of a periodical perturbation. Finally, conclusions are summarized in Section 4.

2. Testing configuration and results post-processing

The characteristics of the 32 different rotors analyzed in the present work are included in Table 1. 26 rotors were equipped with conical cups (90° cone-angle, 4 with cup radius: R_c = 20 mm, cup center rotation radius varying from R_{rc} = 30 mm to R_{rc} = 60 mm; 5 with cup radius: R_c = 25 mm, cup center rotation radius varying from R_{rc} = 40 mm to R_{rc} = 100 mm; 6 with cup radius: R_c = 30 mm, cup center rotation radius varying from R_{rc} = 40 mm to R_{rc} = 120 mm; 5 with cup radius: R_c = 35 mm, cup center rotation radius varying from R_{rc} = 50 mm to R_{rc} = 120 mm; and 6 with cup radius: R_c = 40 mm, cup center rotation radius varying from R_{rc} = 60 mm to R_{rc} = 140 mm). 3 rotors were equipped with elliptical cups (front surface equal to the conical cups: S_c = 1963.5 mm^2 and R_{rc} = 60 mm). And finally, 3 rotors were equipped with porous cups (front surface, including the empty area, equal to the conical cups: S_c = 1963.5 mm^2, cup radius: R_c = 25 mm, truncated shape with hole diameter h = 9 mm, h = 19 mm and h = 24 mm, and R_{rc} = 60 mm). See in Fig. 3 a sketch of the rotor cups tested.

A second testing round, devoted to analyze the effect of rotor non-symmetries on the anemometers' response, was carried out using the h-19/60 rotor as a base configuration. This rotor was calibrated 4 more times, one repeating the calibration of the first testing round, and the other three replacing one of the cups with a cup from the h-09/60, h-24/60 and c-25/60 rotors (see Fig. 4).

The cups were made of ABS plastic using a 3D printer, and the arm on each cup was made of aluminum tubing 5 mm in diameter. In Table 1, the weight, W, and the moment of inertia, I, corresponding to each rotor have been also included. The moment of inertia was calculated for each case adding the contributions of the head of the rotor, the arms and the cups. The moment of inertia of the cups was calculated with the CAD program used for their design. In Fig. 5 the calculated moments of inertia are plotted as a function of the squared cup radius multiplied by the squared cup center rotation radius, $R_c^2 R_{rc}^2$. The experimentally measured moments of inertia of several rotors from commercial anemometers [25,59–61] have been also included in the graph (see also in Table 2 the mass and geometrical characteristics of these rotors). It can be observed in the aforementioned figure that the calculated moments of inertia regarding the rotors tested seem to be quite similar to the ones experimentally measured. The moment of inertia has proven to be of great importance in relation to the anemometers performance. Anemometers with damaged rotors not only can have different aerodynamic behavior [62], a different performance can be shown due to changes on the moment of inertia if one cup is missing or damaged [32,62]. Due to this reason it is relevant to highlight that the testing rotors have both similar geometry and moment of inertia when compared to commercial anemometers.

The testing campaign whose results are analyzed in the present work was carried out using a Climatronics 100075 anemometer, which gives 30 squared pulses per turn. In Fig. 6, a plot of the output signal recorded in one turn of this anemometer equipped with the h-24/60 rotor is shown. The corresponding non-dimensional rotation speed, ω/ω_0, is also included in the figure. It was calculated

Table 1
Geometrical, weight and inertia characteristics of the rotors tested: cup center rotation radius, R_{rc}, front area of the cups, S_c, cup radius (conical and porous cups), R_c, ratio of cup radius to the cups' center rotation radius (conical cups), R_c/R_{rc}, weight of the rotor, W, moment of inertia of the rotor, I, hole diameter of porous cups, h, and semi-major and semi-minor axes, a and b, of elliptical cups. See also Fig. 3.

Rotor	R_c (mm)	S_c (mm^2)	R_{rc} (mm)	R_c/R_{rc}	W (kg)	I (kg m^2)
Conical cups						
c-20/30	20	1256.6	30	0.667	1.73×10^{-2}	9.63×10^{-6}
c-20/40	20	1256.6	40	0.500	1.78×10^{-2}	1.60×10^{-5}
c-20/50	20	1256.6	50	0.400	1.82×10^{-2}	2.44×10^{-5}
c-20/60	20	1256.6	60	0.333	1.87×10^{-2}	3.50×10^{-5}
c-25/40	25	1963.5	40	0.625	2.49×10^{-2}	2.99×10^{-5}
c-25/50	25	1963.5	50	0.500	2.54×10^{-2}	4.49×10^{-5}
c-25/60	25	1963.5	60	0.417	2.59×10^{-2}	6.33×10^{-5}
c-25/80	25	1963.5	80	0.313	2.68×10^{-2}	1.11×10^{-4}
c-25/100	25	1963.5	100	0.250	2.78×10^{-2}	1.74×10^{-4}
c-30/40	30	2827.4	40	0.750	3.54×10^{-2}	5.29×10^{-5}
c-30/50	30	2827.4	50	0.600	3.59×10^{-2}	7.75×10^{-5}
c-30/60	30	2827.4	60	0.500	3.64×10^{-2}	1.08×10^{-4}
c-30/80	30	2827.4	80	0.375	3.74×10^{-2}	1.85×10^{-4}
c-30/100	30	2827.4	100	0.300	3.84×10^{-2}	2.87×10^{-4}
c-30/120	30	2827.4	120	0.250	3.94×10^{-2}	4.13×10^{-4}
c-35/50	35	3848.5	50	0.700	5.06×10^{-2}	1.33×10^{-4}
c-35/60	35	3848.5	60	0.583	5.11×10^{-2}	1.80×10^{-4}
c-35/80	35	3848.5	80	0.438	5.21×10^{-2}	2.99×10^{-4}
c-35/100	35	3848.5	100	0.350	5.30×10^{-2}	4.53×10^{-4}
c-35/120	35	3848.5	120	0.292	5.40×10^{-2}	6.44×10^{-4}
c-40/50	40	5026.5	50	0.800	7.00×10^{-2}	1.89×10^{-4}
c-40/60	40	5026.5	60	0.667	7.05×10^{-2}	2.57×10^{-4}
c-40/80	40	5026.5	80	0.500	7.15×10^{-2}	4.31×10^{-4}
c-40/100	40	5026.5	100	0.400	7.25×10^{-2}	6.56×10^{-4}
c-40/120	40	5026.5	120	0.333	7.35×10^{-2}	9.32×10^{-4}
c-40/140	40	5026.5	140	0.286	7.45×10^{-2}	1.26×10^{-3}
Rotor	a (mm)	b (mm)	S_c (mm^2)	R_{rc} (mm)	W (kg)	I (kg m^2)
Elliptical cups						
a-27/60	27	23.15	1963.5	60	2.53×10^{-2}	6.43×10^{-5}
a-30/60	30	20.83	1963.5	60	2.48×10^{-2}	6.57×10^{-5}
a-35/60	35	17.86	1963.5	60	2.24×10^{-2}	6.80×10^{-5}
Rotor	R_c (mm)	S_c (mm^2)	R_{rc} (mm)	h (mm)	W (kg)	I (kg m^2)
Porous cups						
h-9/60	25	1963.5	60	9	2.26×10^{-2}	5.38×10^{-5}
h-19/60	25	1963.5	60	19	2.05×10^{-2}	5.36×10^{-5}
h-24/60	25	1963.5	60	24	1.73×10^{-2}	5.32×10^{-5}

averaging groups of 30 pulses (one revolution), from the recorded data at every point (that is, at every wind flow velocity) of each performed calibration.

The calibrations were carried out at the IDR/UPM Institute, in the S4 wind tunnel. This facility is an open-circuit wind tunnel with a closed test section measuring 0.9 by 0.9 m. It is served by four 7.5 kW fans with a flow uniformity under 0.2% in the testing area. More details concerning the facility and the calibration process are included in reference [8]. The uncertainty levels of the calibrations performed at the S4 calibration wind tunnel are specified following the ISO/IEC 17025 standard [63], this levels being 0.1 m s^{-1} for wind speeds from 4 m s^{-1} to 10 m s^{-1}, and 0.01V m s^{-1} for wind speeds, V, from 10 m s^{-1} to 23 m s^{-1}. The calibrations studied in the present work were performed following the MEASNET [20,21] recommendations (over 13 points and from 4 m s^{-1} to 16 m s^{-1} wind speed). In each point (wind speed) of every calibration performed, the anemometer's output was sampled during 20 s at 10,000 Hz. In Table 3 the results of the calibrations that were carried out are included.

The first nine harmonic terms of the Fourier expansion (expression (15)) were calculated in every case (each rotor tested and every wind speed during its calibration) upon the non-dimensional rotation speed that, as said, was obtained averaging the data from several revolutions (i.e., groups of 30 pulses). See in Fig. 7 (left) the non-dimensional first and third harmonic terms (ω_1/ω_0 and ω_3/ω_0, respectively), calculated at every point of the calibration performed to the rotor h-19/60. In order to characterize the rotor performance, averaged values of the non-dimensional first and the third harmonic terms, $\bar{\omega}_1$ and $\bar{\omega}_3$, were calculated with data from the 13 points of the calibration procedure:

$$\bar{\omega}_1 = \frac{1}{13}\sum_{j=1}^{13}\left.\frac{\omega_1}{\omega_0}\right|_j, \quad \bar{\omega}_3 = \frac{1}{13}\sum_{j=1}^{13}\left.\frac{\omega_3}{\omega_0}\right|_j, \tag{17}$$

together with the corresponding standard deviations, σ_1 and σ_3, calculated using the general procedure:

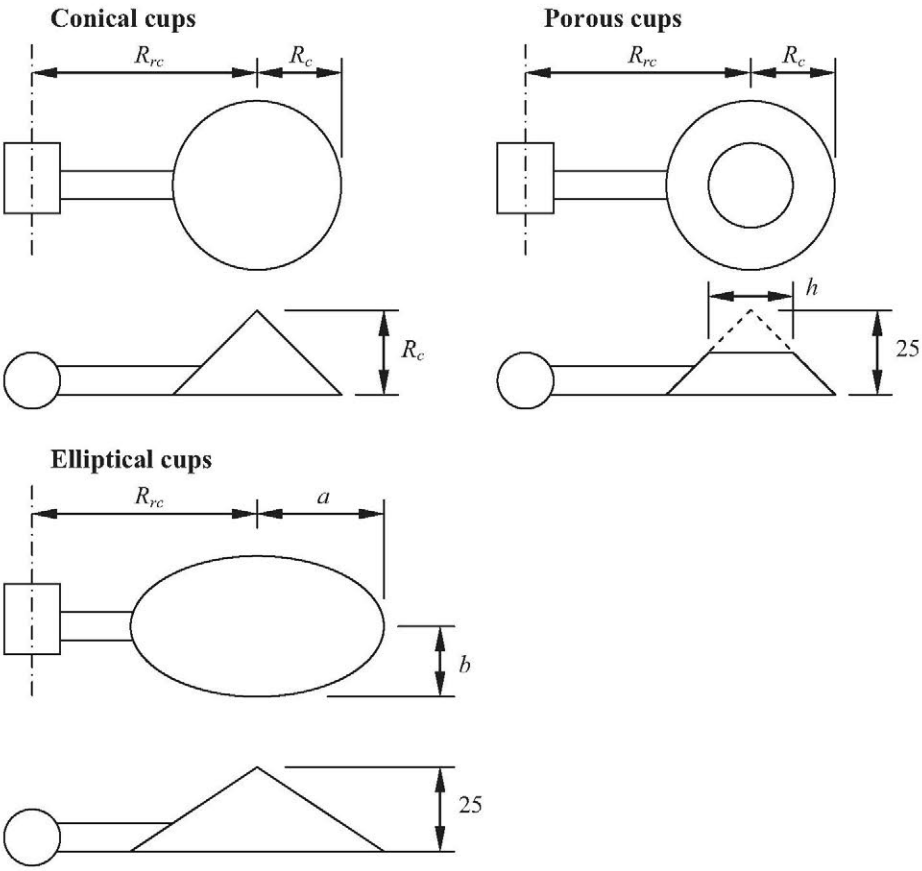

Fig. 3. Sketch of the cups and rotor geometries tested. Dimensions in mm. See also Table 1.

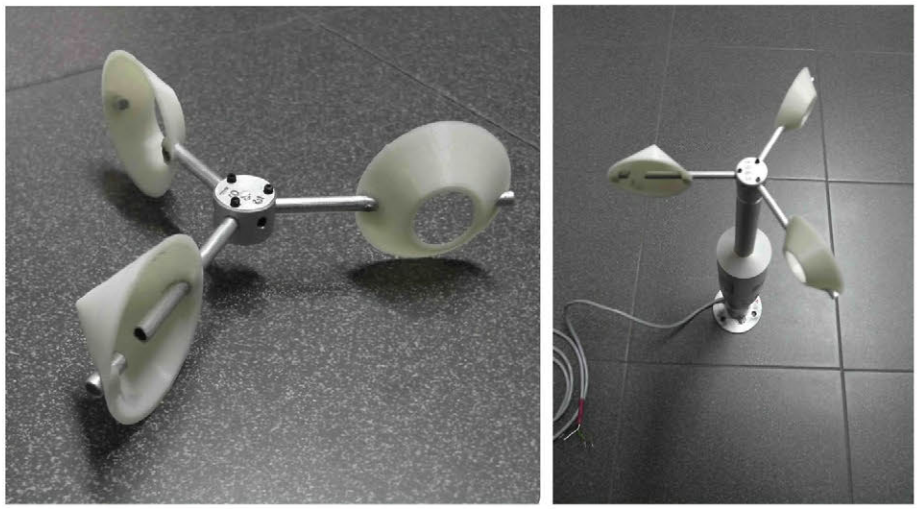

Fig. 4. Pictures of one of the non-axially symmetrical rotors tested (2 cups h-19/60; 1 cup c-25/60). Rotor isolated (left); and installed on the Climatronics 100075 anemometer (right).

$$\sigma_1 = \sqrt{\frac{\sum_{j=1}^{13}\left(\frac{\omega_1}{\omega_0}\Big|_j - \bar{\omega}_1\right)^2}{13-1}},\ \sigma_3 = \sqrt{\frac{\sum_{j=1}^{13}\left(\frac{\omega_3}{\omega_0}\Big|_j - \bar{\omega}_3\right)^2}{13-1}}. \quad (18)$$

The above parameters are also indicated in Fig. 7 (left). The first nine averaged non-dimensional harmonic terms calculated with the procedure above described for rotors c-25/60, h-09/60, h-19/60, and h-24/60 are included in

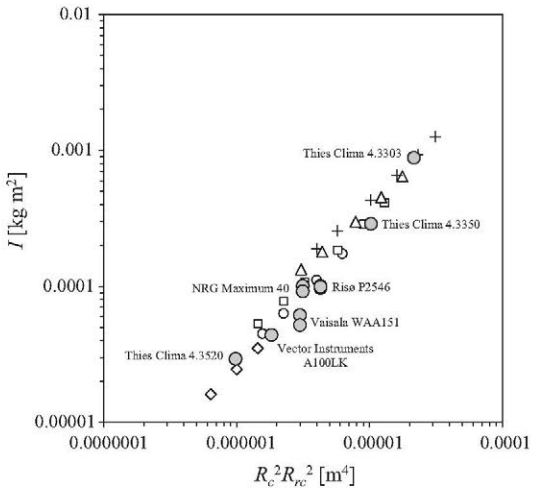

Fig. 5. Moment of inertia, I, of the conical cup rotors tested as a function of the squared cup radius multiplied by the squared cup center rotation radius, $R_c^2 R_{rc}^2$. The results correspond to rotors equipped with $R_c = 20$ (rhombi), 25 (circles), 30 (squares), 35 (triangles), and 40 (crosses) mm cups (see Table 1). Gray circles correspond to different commercial anemometer rotors (see Table 2).

Fig. 7 (right). As expected, the highest figures correspond to the third, sixth and ninth harmonic terms, together with the first one, which is very similar in the four cases included in the figure.

3. Results and discussion

3.1. Experimental results

In Table 3 and Figs. 8 and 9, the results correspondent to the calibrations performed on the conical-cup rotors are included. In Fig. 8 the anemometer factor, K, calculated leaving aside the calibration offset (see expression (8)), is shown as a function of the ratio of cup radius to the cup center rotation radius, $r_r = R_c/R_{rc}$. On the other hand, the graphs contained in Fig. 9 show respectively the first and the third averaged harmonic terms of the rotation, $\bar{\omega}_1$ and $\bar{\omega}_3$, (just called first and third harmonic terms hereinafter), and the correspondent normalized standard deviations, $\sigma_1/\bar{\omega}_1$ and $\sigma_3/\bar{\omega}_3$, as a function of the ratio of cup radius to the cup center rotation radius, $r_r = R_c/R_{rc}$. The data corresponding to calibrations performed to 3 Class-1 new and not calibrated before anemometers (Thies Clima 4.3351; Vector Instruments A100 L2; and Vaisala WAA 151), have been also included in the graphs. The results from a calibration performed to the anemometer used in the present testing campaigns, the Climatronics 100075 anemometer, equipped with its original rotor are also included in the aforementioned figure graphs.

The effect of the ratio of cup radius to the cup center rotation radius, r_r, on the anemometer factor, K, has been analyzed and largely discussed [13–16,24,65]. Nevertheless, it should be pointed out that, leaving aside primary geometrical parameters of the rotor such as the cup radius, R_c, and the cup center rotation radius, R_{rc}, some other shape parameters as the cone angle of the cups, the cup edges (beaded or not, sharp or blunt...), the anemometer "neck" diameter... seem to have some relevance on anemometer performance. It can be observed in Fig. 8 that, in comparison with the conical cup rotors manufactured for the present testing campaign, the commercial anemometers tested and the Climatronics 100075 anemometer equipped with the original rotor have lower values of K, being more efficient in terms of transforming the wind speed into rotational speed (i.e. for the same wind speed, V, higher values of the rotational speed, ω, are reached). The only exception, the Vector Instruments A100 L2 anemometer, has a similar performance in terms of anemometer factor to the manufactured rotors.

Concerning the first harmonic term, $\bar{\omega}_1$, higher values of this parameter are clearly shown by the Climatronics 100075 anemometer (considering all rotors tested, included the original one), when compared to the ones corresponding to the 3 Class-1 new anemometers tested. As already indicated in the introduction of the present work, the first harmonic term is related to all physical effects that are repeated with a period of one turn. These effects are caused by both friction and aerodynamic forces on the rotor. If now the results corresponding to the third harmonic term, $\bar{\omega}_3$, which is directly related to the aerodynamic forces on each cup [15], are examined, it can be observed that no big differences are shown among the data

Table 2
Geometrical characteristics of different commercial anemometer rotors: cup center rotation radius, R_{rc}, front area of the cups, S_c, cup radius, R_c, ratio of cup radius to the cup center rotation radius (conical cups), R_c/R_{rc}, and moment of inertia of the rotor, I.

Anemometer	R_c (mm)	S_c (mm^2)	R_{rc} (mm)	R_c/R_{rc}	W (kg)	I (kg m^2)
Risø P2546	35	3848	59	0.593	5.8×10^{-2} [59]	9.74×10^{-5} [25,59]
						1.01×10^{-4} [64]
						9.92×10^{-5} [61]
Thies Clima 4.3303	39	4778	119	0.328	9.6×10^{-2} [59]	8.87×10^{-4} [25,59]
Thies Clima 4.3520	22	1521	45	0.489	–	2.93×10^{-5} [25]
Thies Clima 4.3350	40	5027	80	0.500	–	2.89×10^{-4} [61]
Vaisala WAA151	27	2290	64	0.422	3.9×10^{-2} [59]	6.14×10^{-5} [61]
						5.2×10^{-5} [59]
NRG Maximum 40	25.5	2043	69.5	0.367	–	1.01×10^{-4} [61]
						9.2×10^{-5} [59]
Vector Instruments A100LK	25	1964	54	0.463	–	4.40×10^{-5} [61]

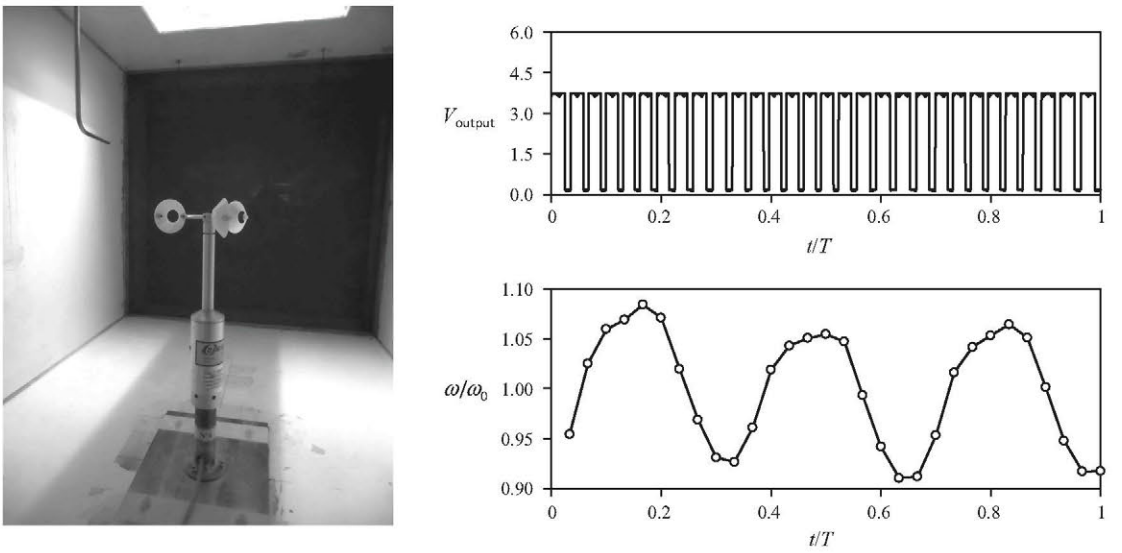

Fig. 6. Climatronics 100075 anemometer placed in the S4 wind tunnel of the IDR/UPM Institute, to carry out a calibration equipped with a porous-cups rotor (left). Anemometer output signal, V_{output}, measured in one turn (right-top). Relative-to-the-average rotational speed, ω/ω_0, calculated in that turn (right-bottom). T is the period of the anemometer's rotation [15].

related to the calibrations performed to the Climatronics 100075 anemometer and the 3 other performed to the new Class-1 anemometers. Based on this fact, it can be assumed that the differences between the Climatronics 100075 anemometer and the new ones regarding the first harmonic term are directly related to the friction effects which, taking into account the large uptime of this anemometer [11], can be attributed to a certain level of degradation regarding the bearings system.

Results indicate the same trend of both the third harmonic, $\bar{\omega}_3$, and the anemometer factor, K, that is, lower values of parameter r_r imply greater values of K and $\bar{\omega}_3$, the pattern being similarly linear. This correlation between the anemometer factor and the third harmonic indicates higher rotational speeds of rotors with lower third harmonic values. This particular behavior has been checked with the rotors with porous and elliptical cups. In Fig. 10 the anemometer constant, K, and the third and first harmonic terms, $\bar{\omega}_3$ and $\bar{\omega}_1$, regarding these rotors have been plotted as a function of the eccentricity, $e = \sqrt{1-(b/a)^2}$, in the case of the elliptical cups, and as a function of the ratio of the hole diameter to the cup diameter, $h/2R_c$, in the case of the porous cups. In the graphs of this figure the results of c-25/60 rotor have been included, as it represents the "zero" case in terms of eccentricity and hole diameter (i.e., $e = 0$ and $h/2R_c = 0$), for the elliptical and porous cup rotors respectively. It should be underlined that all these rotors are characterized by the same cups center rotation radius, $R_{rc} = 60$ mm, and cups with the same front area, $S_c = 1963.5$ mm. For both cases, elliptical and porous cups, the same pattern regarding the anemometer factor, K, and the third harmonic term, $\bar{\omega}_3$, which is in tune with the commented result related to the conical cups, can be observed in Fig. 10. Finally, very similar values of the first harmonic term, $\bar{\omega}_1$, are shown in all these cases, indicating a much greater correlation of this parameter with the mechanical behavior of the anemometer than with the rotor aerodynamics.

Additionally, some conclusions can be extracted from the testing results in relation to the effect of the moment of inertia, I, on the anemometer performance (see Fig. 11). No effect of this parameter has been observed on the first harmonic term, $\bar{\omega}_1$. On the other hand, if both the anemometer factor, K, and the third harmonic term, $\bar{\omega}_3$, are plotted as a function of the moment of inertia (see Fig. 11), it can be clearly observed the effect of the size of the cups and the moment of the inertia. If the value of the rotor's moment of inertia is constant, bigger cups (i.e., larger values of the cup radius, R_c) logically produce lower values of both the anemometer factor, K, and the third harmonic term, $\bar{\omega}_3$, as the aerodynamic forces are increased. Reversely, for constant cups size (i.e., maintaining constant the aerodynamic forces), higher values of the rotor's moment of inertia result in higher values of the anemometer factor, K, and the third harmonic term, $\bar{\omega}_3$.

3.2. Modeling the cup anemometer steady behavior under optimal working conditions (i.e., anemometer not affected by degradation)

The equation that defines the 3-cup model (4), can be expressed as:

$$I\frac{d\omega}{dt} = f(\theta) + f(\theta + 120^\circ) + f(\theta + 240^\circ) \tag{19}$$

where

Table 3
Calibration coefficients, A and B, measured for the rotors tested with a Climatronics 100075 anemometer (see also Table 1). The coefficient of determination, R^2, of the curve fittings, and the slope of the transfer function based on the rotation frequency, A_r (see expressions (1) and (2)), have also been included.

Rotor	A (m/pulse)	A_r (m/rev)	B (m/s)	R^2	$\bar{\omega}_1$ (%)	$\bar{\omega}_3$ (%)
Conical cups						
c-20/30	0.02021	0.60618	0.37096	0.99995	1.22	0.51
c-20/40	0.03177	0.95318	0.23328	0.99999	1.28	0.84
c-20/50	0.04186	1.25574	0.31148	0.99999	1.24	1.09
c-20/60	0.05180	1.55401	0.40091	0.99999	1.33	1.43
c-25/40	0.02963	0.88886	0.26760	0.99999	1.24	0.63
c-25/50	0.03932	1.17970	0.20786	0.99999	1.21	0.92
c-25/60	0.04961	1.48829	0.24245	0.99999	1.30	1.07
c-25/80	0.06964	2.08928	0.39438	0.99999	1.12	1.58
c-25/100	0.08952	2.68552	0.53685	0.99999	1.24	1.78
c-30/40	0.02861	0.85818	0.09551	0.99995	1.24	0.64
c-30/50	0.03861	1.15844	0.19606	0.99999	1.17	0.82
c-30/60	0.04850	1.45505	0.14823	0.99998	1.29	0.99
c-30/80	0.06836	2.05089	0.25403	1.00000	1.34	1.37
c-30/100	0.08697	2.60900	0.38253	0.99998	1.33	1.56
c-30/120	0.10738	3.22145	0.49053	0.99999	1.26	1.74
c-35/50	0.03720	1.11603	0.19081	0.99999	1.20	0.65
c-35/60	0.04719	1.41582	0.15354	0.99999	1.27	0.94
c-35/80	0.06827	2.04818	0.18132	0.99998	1.45	1.15
c-35/100	0.08737	2.62111	0.22168	0.99999	1.14	1.49
c-35/120	0.10742	3.22259	0.34171	0.99999	1.38	1.58
c-40/50	0.03539	1.06166	0.13714	0.99999	1.29	0.52
c-40/60	0.04586	1.37587	0.16652	0.99999	1.27	0.77
c-40/80	0.06663	1.99876	0.16932	0.99998	1.13	1.07
c-40/100	0.08668	2.60026	0.23292	0.99996	1.30	1.34
c-40/120	0.10638	3.19140	0.28805	0.99996	1.20	1.51
c-40/140	0.12639	3.79164	0.34162	0.99995	1.59	1.57
Rotor	A (m/pulse)	A_r (m/rev)	B (m/s)	R^2	$\bar{\omega}_1$ (%)	$\bar{\omega}_3$ (%)
Elliptical cups						
a-27/60	0.05221	1.56617	0.19932	0.99999	1.30	1.39
a-30/60	0.05306	1.59167	0.23224	0.99998	1.25	1.65
a-35/60	0.05412	1.62361	0.21593	0.99998	1.20	2.19
Rotor	A (m/pulse)	A_r (m/rev)	B (m/s)	R^2	$\bar{\omega}_1$ (%)	$\bar{\omega}_3$ (%)
Porous cups						
h-09/60	0.05445	1.63352	0.31414	0.99999	1.16	1.49
h-19/60	0.06579	1.97376	0.54539	0.99998	1.36	2.89
h-24/60	0.11763	3.52881	0.31563	0.99998	1.21	7.56
Rotor	A (m/pulse)	A_r (m/rev)	B (m/s)	R^2	$\bar{\omega}_1$ (%)	$\bar{\omega}_3$ (%)
Non-axially symmetrical rotors (second testing round)						
3 cups h-19/60 (h-19/60 rotor)	0.06573	1.97182	0.55336	0.99998	0.84	2.99
2 cups h-19/60; 1 cup h-24/60	0.07594	2.27822	0.51719	0.99998	5.53	3.93
2 cups h-19/60; 1 cup h-09/60	0.06101	1.83019	0.46162	1.00000	3.12	2.39
2 cups h-19/60; 1 cup c-25/60	0.05831	1.74939	0.40916	0.99999	3.56	2.04

$$f(\theta) = \frac{1}{2}\rho S_c R_{rc}(V^2 + (\omega R_{rc})^2 - 2\omega R_{rc} V\cos(\theta))c_N(\theta)$$
$$= \frac{1}{2}\rho S_c R_{rc}((V^2 + (\omega R_{rc})^2)c_N(\theta) - 2\omega R_{rc} V c_N(\theta)\cos(\theta)). \quad (20)$$

Taking into account Eqs. (9) and (10), together with some trigonometric formulae,[6] the aerodynamic normal force coefficient can be expressed as:

$$c_N(\theta) = \left(c_0 + c_1\eta_0 + \frac{1}{2}c_1\eta_2\right) + \left(c_1\eta_1 + \frac{3}{4}c_1\eta_3\right)\cos(\theta) + \frac{1}{2}c_1\eta_2\cos(2\theta) + \frac{1}{4}c_1\eta_3\cos(3\theta), \quad (21)$$

[6] $\cos^2(\theta) = \frac{1}{2} + \frac{1}{2}\cos(2\theta)$; $\cos^3(\theta) = \frac{3}{4}\cos(\theta) + \frac{1}{4}\cos(3\theta)$.

and then:

$$c_N(\theta)\cos(\theta) = \left(\frac{1}{2}c_1\eta_1 + \frac{3}{8}c_1\eta_3\right) + \left(c_0 + c_1\eta_0 + \frac{3}{4}c_1\eta_2\right)\cos(\theta) + \left(\frac{1}{2}c_1\eta_1 + \frac{1}{2}c_1\eta_3\right)\cos(2\theta) + \frac{1}{4}c_1\eta_2\cos(3\theta) + \frac{1}{8}c_1\eta_3\cos(4\theta). \quad (22)$$

With the above equation, the expression that describes the rotational movement of the rotor can be rewritten as:

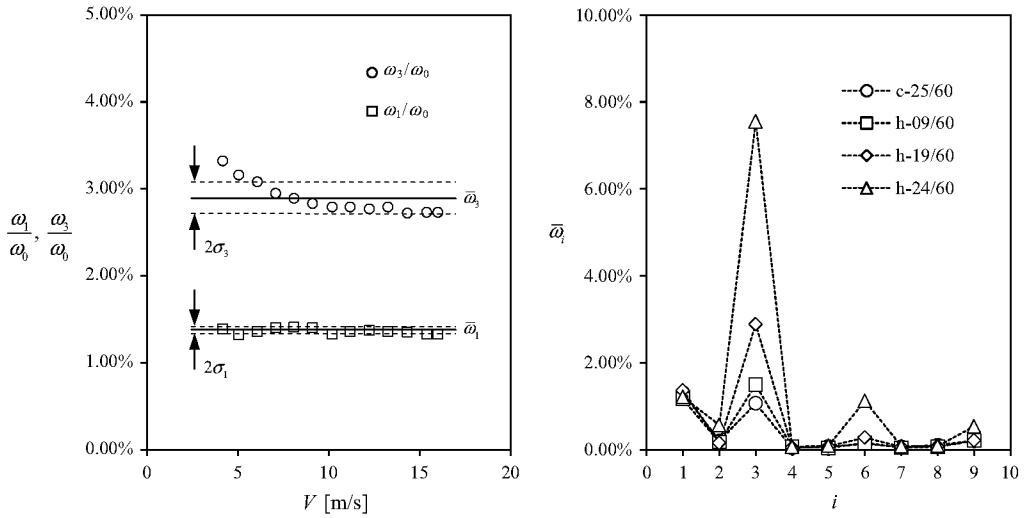

Fig. 7. Non-dimensional first and third harmonic terms, ω_1/ω_0 and ω_3/ω_0, calculated at every point of the calibration performed on the testing anemometer equipped with h-19/60 rotor (left), the average values, $\bar{\omega}_1$ and $\bar{\omega}_3$, and the standard deviations, σ_1 and σ_3, are also indicated in the graph; and (right) first nine averaged non-dimensional harmonic terms, $\bar{\omega}_i = \omega_i/\omega_0$ ($i = 1$ to 9), calculated for rotors c-25/60, h-09/60, h-19/60, and h-24/60 (see also expression (24)).

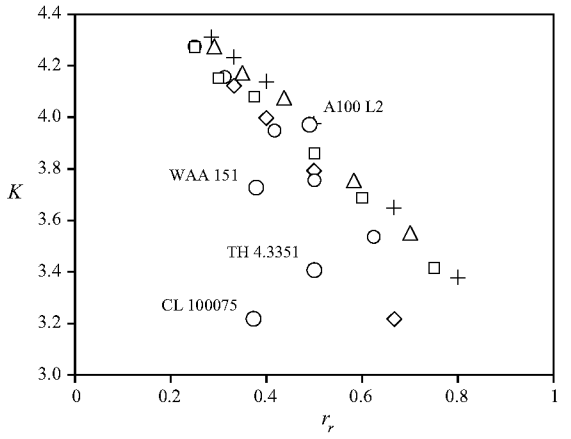

Fig. 8. Anemometer factor, K, corresponding to calibrations performed on a Climatronics 100075 anemometer equipped with different conical-cup rotors as a function of the ratio of cup radius to the cup center rotation radius, $r_r = R_c/R_{rc}$. The symbols stand for the following cup radius: $R_c = 20$ mm (rhombi), 25 mm (circles), 30 mm (squares), 35 mm (triangles), and 40 mm (crosses). Gray circles correspond to results from calibrations performed to new 3 Class-1 anemometers (Thies Clima 4.3351; Vector Instruments A100 L2; Vaisala WAA 151), and the Climatronics 100075 anemometer equipped with its original rotor.

$$\frac{I}{\frac{3}{2}\rho S_c R_{rc}}\frac{\mathrm{d}\omega}{\mathrm{d}t} = \left(V^2 + (\omega R_{rc})^2\right)\left(c_0 + c_1\eta_0 + \frac{1}{2}c_1\eta_2\right) - \omega R_{rc} V\left(c_1\eta_1 + \frac{3}{4}c_1\eta_3\right) + \left(\left(V^2 + (\omega R_{rc})^2\right)\frac{1}{4}c_1\eta_3 - \omega R_{rc} V\frac{1}{2}c_1\eta_2\right)\cos(3\theta), \tag{23}$$

and finally, introducing the anemometer factor, K, in the above expression:

$$\frac{I}{\frac{3}{2}\rho S_c R_{rc} V^2}\frac{\mathrm{d}\omega}{\mathrm{d}t} = \left(\left(1 + \frac{1}{K^2}\right)\left(c_0 + c_1\left(\eta_0 + \frac{1}{2}\eta_2\right)\right) - \frac{1}{K}c_1\left(\eta_1 + \frac{3}{4}\eta_3\right)\right) + \left(\left(1 + \frac{1}{K^2}\right)\eta_3 - \frac{2}{K}\eta_2\right)\frac{c_1}{4}\cos(3\theta). \tag{24}$$

If the stationary condition of the anemometer is considered, and taking into account only the third harmonic term of the rotational wind speed (Eq. (16)), the above equation can be rewritten as:

$$-\frac{I3\omega_0\omega_3}{\frac{3}{2}\rho S_c R_{rc} V^2}\sin(3\omega_0 t + \varphi_3) = \left(\left(1 + \frac{1}{K^2}\right)\left(c_0 + c_1\left(\eta_0 + \frac{1}{2}\eta_2\right)\right) - \frac{1}{K}c_1\left(\eta_1 + \frac{3}{4}\eta_3\right)\right) + \left(\left(1 + \frac{1}{K^2}\right)\eta_3 - \frac{2}{K}\eta_2\right)\frac{c_1}{4}\cos(3\theta). \tag{25}$$

The above expression can be decomposed into two equations. The first one:

$$0 = \left(\left(1 + \frac{1}{K^2}\right)\left(c_0 + c_1\left(\eta_0 + \frac{1}{2}\eta_2\right)\right) - \frac{1}{K}c_1\left(\eta_1 + \frac{3}{4}\eta_3\right)\right), \tag{26}$$

has been already mentioned in Section 1 as Eq. (13). As said, it relates the anemometer factor, K, to the Fourier coefficients ratio c_1/c_0, which, as mentioned, only depends on cup aerodynamics [14]. This expression gives then the average rotation speed of the anemometer rotor, ω_0, as a function of the wind speed, the cups center rotation radius,

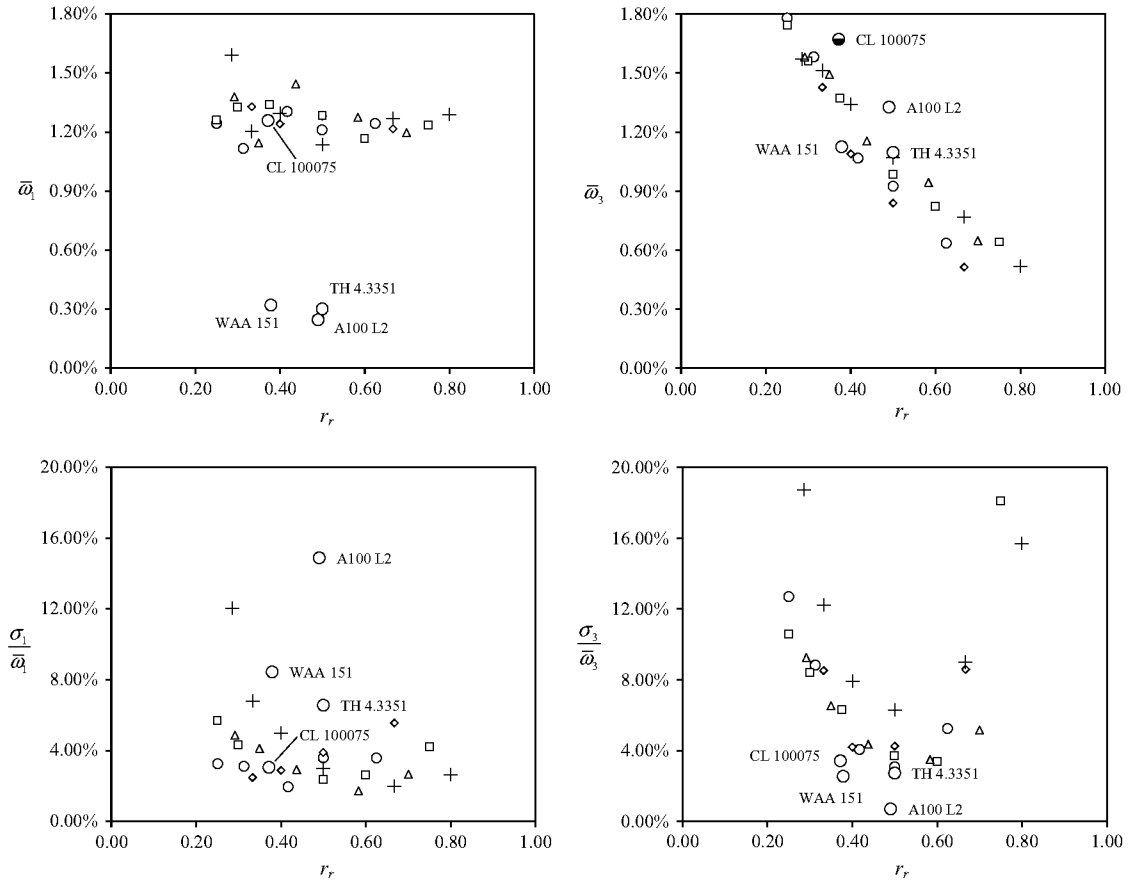

Fig. 9. First and third averaged harmonic terms of the rotation, $\bar{\omega}_1$ and $\bar{\omega}_3$, and correspondent normalized standard deviations, $\sigma_1/\bar{\omega}_1$ and $\sigma_3/\bar{\omega}_3$, as a function of the ratio of cup radius to the cup center rotation radius, $r_r = R_c/R_{rc}$. The results correspond to calibrations performed on a Climatronics 100075 anemometer equipped with $R_c = 20$ (rhombi), 25 (circles), 30 (squares), 35 (triangles), and 40 (crosses) mm cup rotors. Gray circles correspond to results from calibrations performed to three new Class-1 anemometers (Thies Clima 4.3351; Vector Instruments A100 L2; Vaisala WAA 151), and the Climatronics 100075 anemometer equipped with its original rotor.

R_{rc}, and the aerodynamic characteristics of the cup. The linear fitting:

$$K = -0.4147 + 1.5504\frac{c_1}{c_0}, \tag{27}$$

is proved to be a good approximation to Eq. (26) within the range from $c_1/c_0 = 2.25$ ($K = 3$) to $c_1/c_0, = 6.74$ ($K = 10$), where the factors regarding most commercial anemometers lie [14].

On the other hand, the second equation:

$$\frac{I\omega_0\omega_3}{\frac{1}{2}\rho S_c R_{rc} V^2} = \left|\left(\left(1+\frac{1}{K^2}\right)\eta_3 - \frac{2}{K}\eta_2\right)\frac{c_1}{4}\right|, \tag{28}$$

can be derived to an expression formed by dimensionless terms:

$$\frac{\omega_3}{\omega_0} = \bar{\omega}_3 = \left(\frac{\pi}{8}\right)\left|\left((K^2+1)\eta_3 - 2K\eta_2\right)\right|c_1 r_r^2 \Phi, \tag{29}$$

where

$$\Phi = \frac{\rho R_{rc}^5}{I}, \tag{30}$$

is an inertial parameter that represents the ratio between the inertia of a mass of air proportional to anemometer rotor dimensions, and the rotor's inertia. Taking into account the relationship between the anemometer factor, K, and the coefficients ratio, c_1/c_0, stated in Eqs. (26) and (27), it can be assumed that the third term of the equation above depends also on the coefficients ratio c_1/c_0, a reasonable fitting being:

$$(K^2+1)\eta_3 - 2K\eta_2 = 0.5308\left(\frac{c_1}{c_0} - 1\right)^{-1.599} - 0.5, \tag{31}$$

for the bracket between $K = 1.8$ and $K = 10$. The above expression is interesting as it reveals the existence of a theoretical minimum value of the third harmonic term, i.e. $\omega_3/\omega_0 \sim 0$, at a certain value of the coefficients ratio around $c_1/c_0 = 2.05$. It should be underlined that the mentioned coefficients ratio only depends on the cup aerodynamics (see Fig. 1 and expression (9)). Finally, a direct relationship between the non-dimensional third harmonic term, ω_3/ω_0, and the force coefficient c_1 is observed, this result being expected as this coefficient is related to the

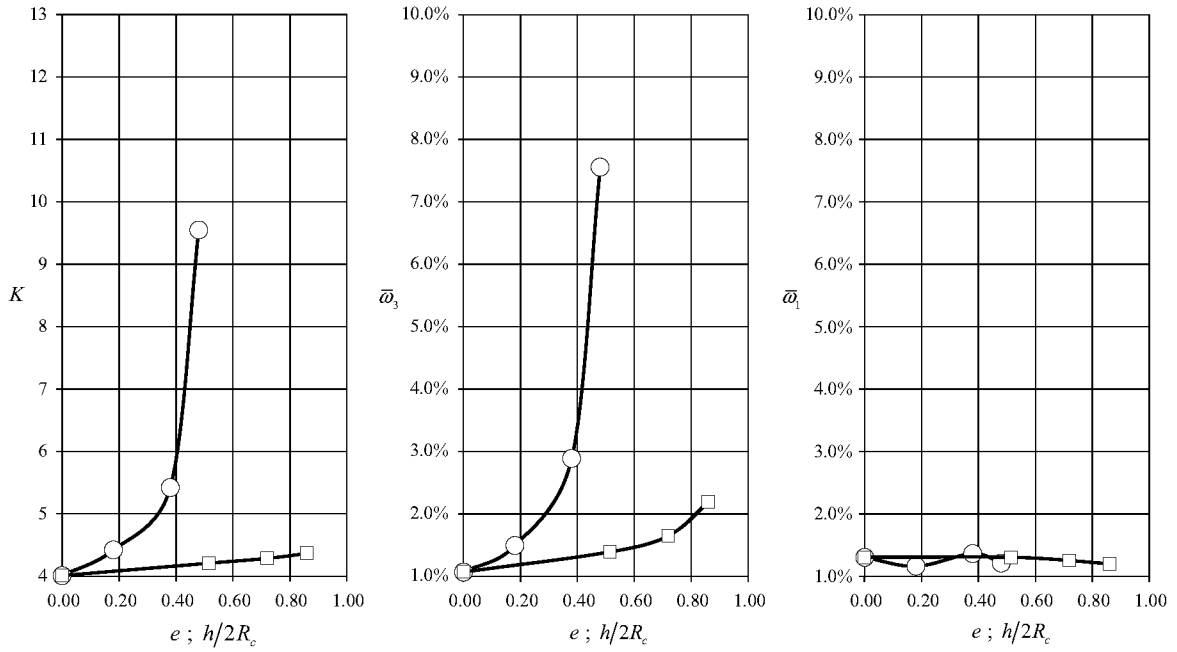

Fig. 10. Anemometer constant, K, and non-dimensional third and first harmonic terms, $\bar{\omega}_3$ and $\bar{\omega}_1$, regarding calibrations performed to the anemometer equipped with elliptical (squares) and porous (circles) cup rotors, as a function of the eccentricity, $e = \sqrt{1-(b/a)^2}$, and the ratio of the hole diameter to the front cup area, $h/2R_c$, respectively.

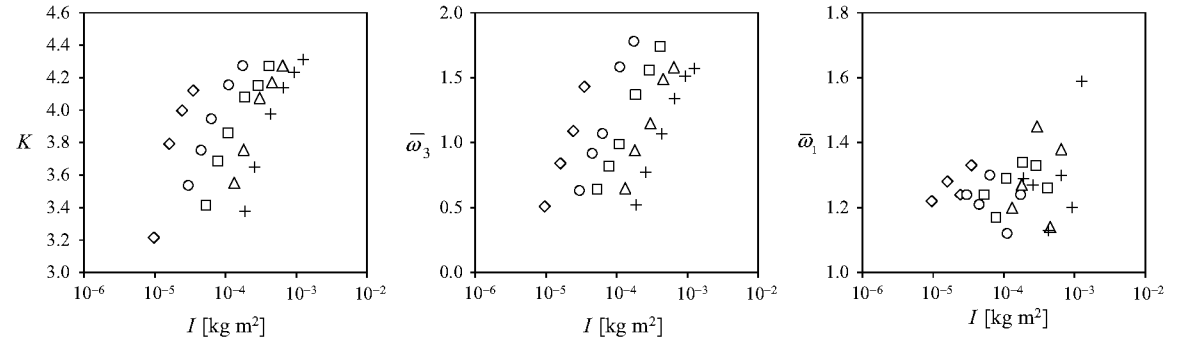

Fig. 11. Anemometer constant, K, and non-dimensional third and first harmonic terms, $\bar{\omega}_3$ and $\bar{\omega}_1$, regarding calibrations performed to the anemometer equipped with conical cup rotors, in relation to the rotor's moment of inertia, I. The results correspond to calibrations performed on a Climatronics 100075 anemometer equipped with $R_c = 20$ (rhombi), 25 (circles), 30 (squares), 35 (triangles), and 40 (crosses) mm cup rotors.

aerodynamic normal force oscillation on each cup in one rotation.

In Table 4 coefficients c_0 and c_1 from the Fourier series correspondent to the normal-to-the-cup force coefficient, c_N (Eq. (9)), are included for the conical (represented by the c-25/60 rotor), porous and elliptical cups. These coefficients were all experimentally measured with the only exception of the h-09/60 rotor cups [14]. In this particular case the coefficients were interpolated from the other testing results. The anemometer factor, K, measured (expression (8)) and calculated (expression (27)) is also included, together with the measured (Table 3) and calculated (Eq. (29)) third harmonic term, $\bar{\omega}_3$. As already stated, the calculated anemometer factor fits reasonably well with experimental results [13,14], although it underestimates the average rotation speed, ω_0, up to a 22% in the worst result of the studied cases. On the other hand, significant differences are observed between the calculated and the measured third harmonic terms. These differences can be explained as the measured third harmonic term values are around 2% of the average rotation speed (a maximum of 7.56% was measured in the extreme case represented by the h-24/60 rotor), which is quite small compared to the deviations found regarding the average rotation speed, ω_0. It seems reasonable to assume larger deviations in the calculated secondary term (i.e., the third harmonic term, ω_3), if the deviation from the primary one (the average rotation speed, ω_0) is greater than the measured value of

Table 4
Aerodynamic cup coefficients c_0 and c_1 from the Fourier series correspondent to the normal-to-the-cup force coefficient, c_N (Eq. (9)), calculated from the conical (represented by the c-25/60 rotor), porous and elliptical cups wind tunnel measurements [14]. The coefficients c_0 and c_1 corresponding to the h-09/60 cups were interpolated as no testing results were available. The anemometer factor, K, and third harmonic term, $\bar{\omega}_3$, calculated upon the aforementioned coefficients and based on the measurements (Table 3) are also included in the table.

Rotor cups	Cup coefficients			Calculated		Measured	
	c_0	c_1	c_1/c_0	K	$\bar{\omega}_3$ (%)	K	$\bar{\omega}_3$ (%)
c-25/60	0.348	1.152	3.312	4.72	0.038	3.95	1.07
h-09/60	0.331	1.147	3.464	4.96	0.047	4.33	1.49
h-19/60	0.235	1.029	4.372	6.36	0.053	5.23	2.89
h-24/60	0.123	0.767	6.240	9.26	0.039	9.36	7.56
a-27/60	0.386	1.225	3.174	4.51	0.039	4.15	1.39
a-30/60	0.367	1.227	3.341	4.77	0.040	4.22	1.65
a-35/60	0.336	1.288	3.832	5.53	0.044	4.31	2.19

the secondary term. In order to analyze this deviation from the testing results, the third harmonic term of the porous and elliptical cup rotors was related to the rotor formed by conical cups (i.e., c-25/60 rotor), the results being included in Fig. 12. As said in the previous section, the c-25/60 rotor represents the "zero" case in terms of eccentricity and hole diameter for the elliptical and porous cup rotors. The analytical method underestimates the effect of the changes on the cups on the compared third harmonic term, although the tendencies seem to be somehow reflected in the graph with the exception of the h-24/60 rotor. Taking into account the reduction in terms of aerodynamic forces on the cups due to its high porosity (see Table 4), the deviation of the h-24/60 rotor could be attributed, in principle, to a higher level of aerodynamic interaction between the rotor cups and the stream formed by the anemometer "neck" and the cups arms (which also have in this case a larger relative contribution to the aerodynamic moment). Moreover, the measured third harmonic terms, $\bar{\omega}_3$, from the conical cup rotors tested are plotted as a function of inertial parameter Φ multiplied by the squared ratio of cup radius to the cup center rotation radius, r_r^2, in

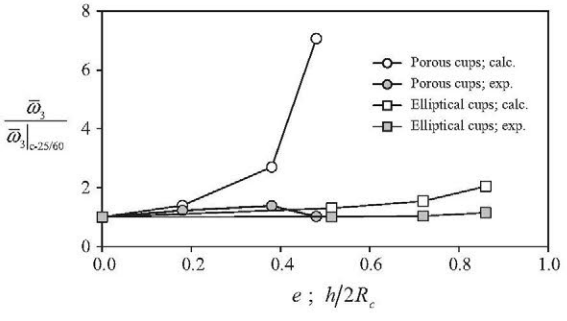

Fig. 12. Third harmonic term of the porous and elliptical cup rotors related to the third harmonic related to the conical cup rotor (c-25/60 rotor), $\bar{\omega}_3/\bar{\omega}_3|_{c-25/60}$, respectively plotted as a function of the non-dimensional hole diameter, $h/2R_c$, and the eccentricity, e, of the cups.

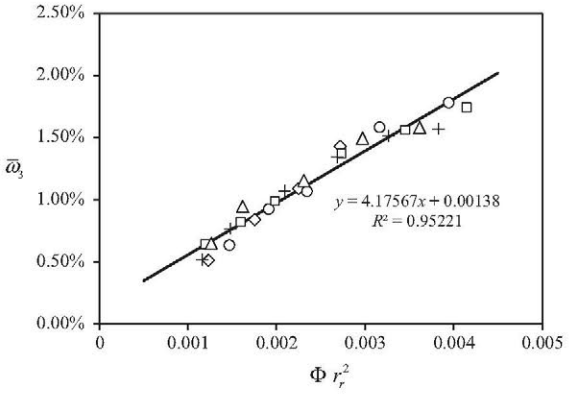

Fig. 13. Measured third harmonic term, $\bar{\omega}_3$, of the conical cup rotors as a function of the inertia parameter, Φ, multiplied by the squared ratio of the cup diameter to the cup center rotation radius, r_r. The symbols stand for the following cup radius: $R_c = 20$ mm (rhombi), 25 mm (circles), 30 mm (squares), 35 mm (triangles), and 40 mm (crosses).

Fig. 13. It can be observed that the results indicate a linear tendency just like the present model does with expression (29). Further improvements should be made to this analytical model in order to have a closer approximation to testing results with regard the third harmonic term. In this sense, recent results indicate that the aerodynamic force on the rotor cups is not uniform due to the rotational movement. The implementation of this effect could probably increase the accuracy of the 3-cup analytical model as it has been done with the 2-cup analytical model [16].

3.3. Modeling the cup anemometer behavior under the effect of a periodical perturbation

As previously mentioned in Section 2, different non-symmetrical rotors were manufactured to study the effect of a periodical perturbation on the anemometer performance. The perturbation on the rotor dynamics is then introduced by modifying the aerodynamic behavior of one cup. This case can occur if one of the cups is damaged as a result of the normal degradation causes of the anemometer (i.e., frost and snow accumulation [33]).

If the 3-cup analytical model is considered to analyze the aerodynamics of a rotor formed by two cups of normal-to-the-cup aerodynamic force coefficient $c_N(\alpha)$, and a third cup of affected coefficient $c_N^*(\alpha)$, the equation of the movement can be rewritten as:

$$I\frac{d\omega}{dt} = f^*(\theta) + f(\theta + 120^\circ) + f(\theta + 240^\circ)$$
$$= f(\theta) + f(\theta + 120^\circ) + f(\theta + 240^\circ) + f'(\theta) \quad (32)$$

where $f(\theta)$, $f(\theta + 120^\circ)$ and $f(\theta + 240^\circ)$ are defined by expression (20) and:

$$f'(\theta) = \frac{1}{2}\rho S_c R_{rc}(V^2 + (\omega R_{rc})^2 - 2\omega R_{rc} V \times \cos(\theta))\Delta c_N(\theta). \quad (33)$$

with, taking into account Eqs. (9) and (10):

$$\begin{aligned}\Delta c_N(\theta) &= c_N{}^*(\theta) - c_N(\theta)\\ &= \left((c_0{}^* - c_0) + (c_1{}^* - c_1)\left(\eta_0 + \frac{1}{2}\eta_2\right)\right)\\ &\quad + (c_1{}^* - c_1)\left(\eta_1 + \frac{3}{4}\eta_3\right)\cos(\theta)\\ &\quad + \frac{1}{2}(c_1{}^* - c_1)\eta_2\cos(2\theta) + \frac{1}{4}(c_1{}^* - c_1)\eta_3\cos(3\theta)\\ &= (\Delta c_0 + \Delta c_1\left(\eta_0 + \frac{1}{2}\eta_2\right)) + \Delta c_1\left(\eta_1 + \frac{3}{4}\eta_3\right)\cos(\theta)\\ &\quad + \frac{1}{2}\Delta c_1\eta_2\cos(2\theta) + \frac{1}{4}\Delta c_1\eta_3\cos(3\theta). \end{aligned} \tag{34}$$

Then, using the same mathematical procedure described in Section 3.1 the following expression can be derived:

$$\begin{aligned}\frac{I}{\frac{3}{2}\rho S_c R_{rc} V^2}\frac{\mathrm{d}\omega}{\mathrm{d}t} &= \left(\left(1 + \frac{1}{K^2}\right)\left(c_0 + c_1(\eta_0 + \frac{1}{2}\eta_2)\right)\right.\\ &\quad \left. - \frac{1}{K}c_1\left(\eta_1 + \frac{3}{4}\eta_3\right)\right)\\ &\quad + \left(\left(1 + \frac{1}{K^2}\right)\eta_3 - \frac{2}{K}\eta_2\right)\frac{c_1}{4}\cos(3\theta)\\ &\quad + G(\Delta c_0; \Delta c_1; K; \theta), \end{aligned} \tag{35}$$

where

$$\begin{aligned}G(\Delta c_0; \Delta c_1; K; \theta) &= \frac{1}{3}\left(1 + \frac{1}{K^2}\right)\left(\Delta c_0 + \Delta c_1\left(\eta_0 + \frac{1}{2}\eta_2\right)\right)\\ &\quad - \frac{1}{3}\frac{1}{K}\left(\Delta c_1\left(\eta_1 + \frac{3}{4}\eta_3\right)\right)\\ &\quad + \frac{1}{3}\left(1 + \frac{1}{K^2}\right)\left(\Delta c_1(\eta_1 + \frac{3}{4}\eta_3)\right)\cos(\theta)\\ &\quad - \frac{1}{3}\frac{1}{K}\left(2\Delta c_0 + \Delta c_1\left(2\eta_0 + \frac{3}{2}\eta_2\right)\right)\cos(\theta)\\ &\quad + \frac{1}{6}\left(1 + \frac{1}{K^2}\right)\Delta c_1\eta_2\cos(2\theta)\\ &\quad - \frac{1}{3}\frac{1}{K}\Delta c_1(\eta_1 + \eta_3)\cos(2\theta)\\ &\quad + \frac{1}{12}\left(1 + \frac{1}{K^2}\right)\Delta c_1\eta_3\cos(3\theta)\\ &\quad - \frac{1}{6}\frac{1}{K}\Delta c_1\eta_2\cos(3\theta) - \frac{1}{12}\frac{1}{K}\Delta c_1\eta_3\cos(4\theta). \end{aligned} \tag{36}$$

Taking into account the above expressions, the steady state equation is now defined by the following equation:

$$\begin{aligned}0 &= \left(\left(1 + \frac{1}{K^2}\right)\left(c_0 + c_1\left(\eta_0 + \frac{1}{2}\eta_2\right)\right) - \frac{1}{K}c_1\left(\eta_1 + \frac{3}{4}\eta_3\right)\right)\\ &\quad + \frac{1}{3}\left(\left(1 + \frac{1}{K^2}\right)\left(\Delta c_0 + \Delta c_1\left(\eta_0 + \frac{1}{2}\eta_2\right)\right) - \frac{1}{K}\Delta c_1\left(\eta_1 + \frac{3}{4}\eta_3\right)\right)\\ &= \left(\left(1 + \frac{1}{K^2}\right)\left(c_0' + c_1'(\eta_0 + \frac{1}{2}\eta_2)\right) - \frac{1}{K}c_1'\left(\eta_1 + \frac{3}{4}\eta_3\right)\right), \end{aligned} \tag{37}$$

where, obviously:

$$c_0' = c_0 + \frac{1}{3}\Delta c_0;\ c_1' = c_1 + \frac{1}{3}\Delta c_1. \tag{38}$$

As said in the previous sections, expression (37) gives a value of the anemometer factor as a function of the ratio c_1'/c_0', which can be approximated by the following expression:

$$\frac{c_0'}{c_1'} = \frac{c_0 + \frac{1}{3}\Delta c_0}{c_1 + \frac{1}{3}\Delta c_1} \approx \frac{c_0}{c_1}\left(1 + \frac{\Delta c_1}{3c_1} - \frac{\Delta c_0}{3c_0}\right). \tag{39}$$

Concerning the first to the fourth harmonic terms, they can be derived from expressions (35) and (36):

$$\begin{aligned}\frac{\omega_1}{\omega_0} = \bar{\omega}_1 &= \left(\frac{\pi}{2}\right)\left|\left((K^2 + 1)\left(\eta_1 + \frac{3}{4}\eta_3\right)\right.\right.\\ &\quad \left.\left. - 2K\left(\frac{\Delta c_0}{\Delta c_1} + \eta_0 + \frac{3}{2}\eta_2\right)\right)\Delta c_1\right| r_r^2\Phi, \end{aligned} \tag{40}$$

$$\frac{\omega_2}{\omega_0} = \bar{\omega}_2 = \left(\frac{\pi}{4}\right)\left|\left((K^2 + 1)\frac{1}{2}\eta_2 - K(\eta_1 + \eta_3)\right)\Delta c_1\right| r_r^2\Phi, \tag{41}$$

$$\begin{aligned}\frac{\omega_3}{\omega_0} = \bar{\omega}_3 &= \left(\frac{\pi}{4}\right)\left|\left((K^2 + 1)\frac{1}{2}\eta_3 - K\eta_2\right)c_1\right.\\ &\quad \left. + \left((K^2 + 1)\frac{1}{6}\eta_3 + \frac{1}{3}K\eta_2\right)\Delta c_1\right| r_r^2\Phi, \end{aligned} \tag{42}$$

$$\frac{\omega_4}{\omega_0} = \bar{\omega}_4 = \left(\frac{\pi}{32}\right)|K\eta_3\Delta c_1| r_r^2\Phi, \tag{43}$$

In Table 5 the results calculated with this model are included together with the testing results. In Fig. 14, the measured and calculated anemometer factor, K, and the first, second and third, $\bar{\omega}_1$, $\bar{\omega}_2$, and $\bar{\omega}_3$, are plotted as a function of percentage variation of the c_0 aerodynamic coefficient regarding the perturbed cup of the non-symmetrical rotor, $\Delta c_0/c_0$. This parameter seems to be a good choice to represent the change of normal-to-the-cup aerodynamic force on the cup, bearing in mind that a completely flat cup which is unable to create aerodynamic moment on the rotor is characterized by $c_0 = 0$ due to its symmetry. The averaged rotational speed, ω_0, characterized by the anemometer factor, K, is, as expected, affected by the change of the aerodynamic force on one of the cups, the factor being lower (i.e., higher rotational speeds) for higher values of the aforementioned aerodynamic force. Also, the results indicate a good correlation between the studied analytical model and the testing results. With regard to the first harmonic term, $\bar{\omega}_1$, the testing results clearly show higher values for the non-symmetrical rotors, with again good correlation with the data resulting from the analytical model.

The second and the third harmonic terms, $\bar{\omega}_2$, and $\bar{\omega}_3$, experimentally measured show a different pattern in comparison with the first one, their values being inversely proportional with the increment of aerodynamic force on the affected cup. With respect to the third harmonic term it should be underlined that, although it decreases with the increase of the aerodynamic force on one cup of the rotor, it cannot be taken as an increase of the rotation speed uniformity due to the higher values of the first harmonic term, $\bar{\omega}_1$. In this case the correlation of the results from the analytical method with the testing results is worse than the

Table 5
Anemometer factor, K, and the first four harmonic terms, $\bar{\omega}_1$, $\bar{\omega}_2$, $\bar{\omega}_3$ and $\bar{\omega}_4$, analytically calculated and measured with the Climatronics 100075 anemometer equipped with non-symmetrical rotors. The description of the rotors (i.e., the cups forming them) and their moment of inertia, I, are included in the table. See also Fig. 4 and Table 3.

Rotor cups	I (kg m^2)	Calculated					Measured				
		K	$\bar{\omega}_1$ (%)	$\bar{\omega}_2$ (%)	$\bar{\omega}_3$ (%)	$\bar{\omega}_4$ (%)	K	$\bar{\omega}_1$ (%)	$\bar{\omega}_2$ (%)	$\bar{\omega}_3$ (%)	$\bar{\omega}_4$ (%)
(2) h-19/60 (1) c-25/60	5.68×10^{-5}	5.688	1.09	0.07	0.044	7.8×10^{-4}	4.640	3.56	0.10	2.04	0.16
(2) h-19/60 (1) h-09/60	5.37×10^{-5}	5.814	1.24	0.07	0.047	6.8×10^{-4}	4.855	3.12	0.15	2.39	0.17
(3) h-19/60	5.36×10^{-5}	6.364	0	0	0.047	0	5.230	0.84	0.22	2.99	0.07
(2) h-19/60 (1) h-24/60	5.35×10^{-5}	6.990	4.85	0.2	0.045	6.8×10^{-4}	6.043	5.53	1.08	3.93	0.34

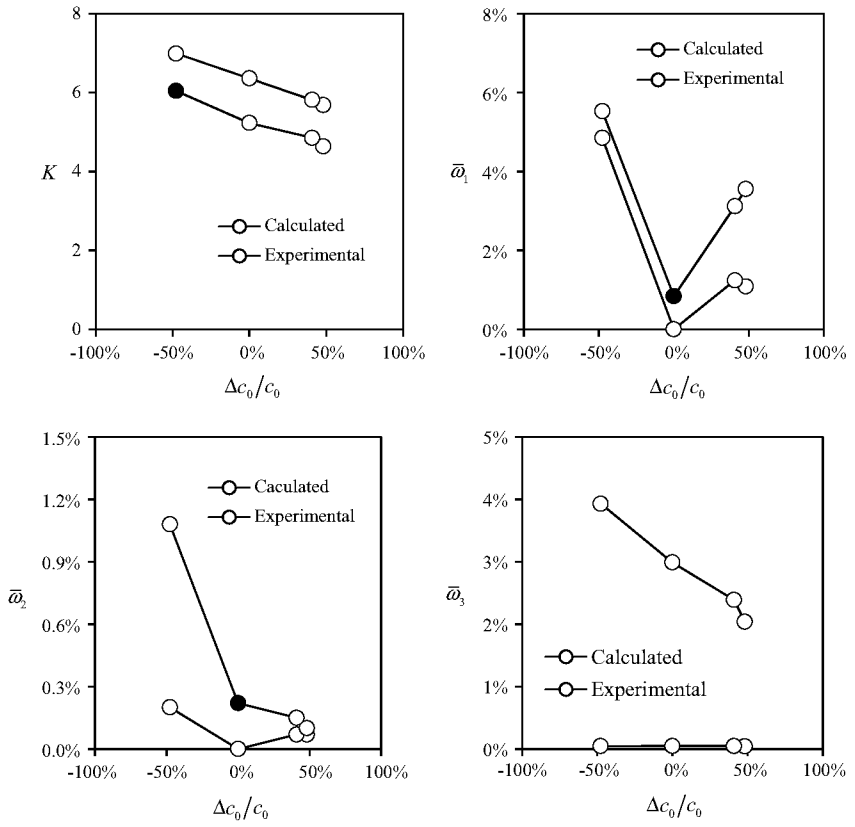

Fig. 14. Results with regard to the performance analysis (experimental and calculated with the proposed analytical model) of the Climatronics 100075 cup anemometer equipped with non-symmetrical rotors (see Fig. 4). Variation of the anemometer factor, K, and the first, second and third, $\bar{\omega}_1$, $\bar{\omega}_2$, and $\bar{\omega}_3$, as a function of the percentage variation of the aerodynamic forces on the perturbed cup of the non-symmetrical rotor, $\Delta c_0/c_0$ (see expressions (9) and (34)).

one described for the anemometer factor and the first harmonic term. More precisely, it seems that in the case of the second harmonic term, $\bar{\omega}_2$, there is some level of correlation measured in the case of a decrease in the aerodynamic force on the affected cup, whereas no correlation between the calculations and the testing results is observed in the case of the third harmonic term, $\bar{\omega}_3$.

4. Conclusions

In the present work, the harmonic terms of cup anemometer rotation speed, ω, and their effects on anemometer performance (on steady wind) are experimentally and analytically studied, with quite good agreement among results from both methodologies. The effect of mechanical perturbations on the anemometer performance has been also analyzed with non-symmetrical rotors. The most relevant conclusions resulting from this work are:

- Anemometers working in normal conditions (i.e., not affected my any mechanical perturbation) show a high correlation level between their aerodynamic efficiency (i.e., the capability of transforming the incoming wind

speed into rotational speed) and the rotation uniformity characterized by the third harmonic term, $\bar{\omega}_3$. Therefore, a more uniform rotation of the anemometer rotor results in higher averaged rotation speed, ω_0.

- Also, the aforementioned third harmonic term, $\bar{\omega}_3$, seems to be more uniform within the calibration speed range (from 4 m s^{-1} to 16 m s^{-1}) for certain rotor sizes, with values of the ratio of cup radius to the cup center rotation radius, $r_r = R_c/R_{rc}$, from $r_r = 0.4$ to $r_r = 0.5$.
- The 3-cup analytical model, even being accurate enough to analyze the effect of the rotor shape on the anemometer factor K (i.e., the averaged rotation speed, ω_0), needs to be further improved to accurately reproduce the third harmonic term of the rotation speed, $\bar{\omega}_3$. Nevertheless, the model was able to correctly indicate some aspects related to this harmonic term such us the linear relationship with the rotor inertia parameter $\Phi = \rho R_{rc}^5/I$. One of the most promising improvements to this 3-cup analytical model could be to consider the pressure distribution on the cups not constant, as some recent results indicate higher aerodynamic pressure coefficient at the area of the cups closer to the rotation axis [16].
- Experimental results clearly indicate higher values of the first harmonic term, $\bar{\omega}_1$, in calibrations carried out on an old anemometer (affected by a certain degree of wear and tear) equipped with different rotors, than the ones related to calibrations performed on new anemometers.
- Anemometers affected by an aerodynamic perturbation on one single cup of the rotor showed, as expected, higher values of the first harmonic term, $\bar{\omega}_1$. Also, the testing results indicated a good correlation among the perturbation and its effect on anemometer aerodynamic performance, that is, an increase of the aerodynamic normal-to-the-cup force coefficient in one of the rotor cups was translated into higher values of rotor aerodynamic efficiency (as said, lower value of anemometer factor, K), whereas a decrease of the aforementioned coefficient resulted in the opposite effect.
- The calculations done using the 3-cup analytical model accurately reproduced the effect of the aforementioned aerodynamic perturbation on one single cup of the rotor.
- Although more testing campaigns focusing specifically on the correlation between the first harmonic term, $\bar{\omega}_1$, and the anemometer degradation due to wear and tear should be carried out, this promising result suggests a new parameter as a key variable in the condition monitoring/diagnosis of cup anemometers.

Acknowledgments

The authors are indebted to Prof. Ángel Sanz Andrés for his encouraging support regarding the research program on cup anemometers performance. The authors are grateful to Anna María Ballester for her kind help on improving the style of the text. Prof. Pindado and the other co-authors are truly indebted to the staff of the Library at the Aeronautics and Space Engineering School (*Escuela de Ingeniería Aeronáutica y del Espacio*) of the Polytechnic University of Madrid (*Universidad Politécnica de Madrid*), for their constant support to the research carried out regarding cup anemometer performances. Finally, the authors would like to dedicate this work to the memory of Prof. José Meseguer, head of the IDR/UPM Institute since its founding, whose wise advice and constant support helped many in their scientific and academic careers.

References

[1] L. Kristensen, Can a cup anemometer "underspeed"? A heretical question, Boundary-Layer Meteorol. 103 (2002) 163–172.
[2] A. Albers, H. Klug, Open field cup anemometry, DEWI Mag. 19 (2001) 53–58.
[3] A. Albers, H. Klug, D. Westermann, Outdoor comparison of cup anemometers, DEWI Mag. 17 (2000) 5–15.
[4] S. Lang, E. McKeogh, LIDAR and SODAR measurements of wind speed and direction in upland terrain for wind energy purposes, Remote Sens. 3 (2011) 1871–1901, http://dx.doi.org/10.3390/rs3091871.
[5] R. Wagner, M. Courtney, J. Gottschall, P. Lindelöw-Marsden, Accounting for the speed shear in wind turbine power performance measurement, Wind Energy 14 (2011) 993–1004.
[6] R.V. Coquilla, J. Obermeier, B.R. White, Calibration procedures and uncertainty in wind power anemometers, Wind Eng. 31 (2007) 303–316.
[7] F. Aminzadeh, S. Pindado, How has Spain become a leader in the wind energy industry during the last decade? (An analysis of influential factors on the development of wind energy in Spain), in: Proc. EWEA Annu. Event. Brussels 2011, 2011.
[8] S. Pindado, E. Vega, A. Martínez, E. Meseguer, S. Franchini, I. Pérez, Analysis of calibration results from cup and propeller anemometers. Influence on wind turbine Annual Energy Production (AEP) calculations, Wind Energy 14 (2011) 119–132, http://dx.doi.org/10.1002/we.407.
[9] L. Kristensen, Cup anemometer behavior in turbulent environments, J. Atmos. Ocean. Technol. 15 (1998) 5–17.
[10] L. Makkonen, P. Lehtonen, L. Helle, Anemometry in icing conditions, J. Atmos. Ocean. Technol. 18 (2001) 1457–1469.
[11] S. Pindado, A. Barrero-Gil, A. Sanz, Cup Anemometers' loss of performance due to ageing processes, and its effect on Annual Energy Production (AEP) estimates, Energies 5 (2012) 1664–1685, http://dx.doi.org/10.3390/en5051664.
[12] S. Pindado, A. Sanz, A. Wery, Deviation of cup and propeller anemometer calibration results with air density, Energies 5 (2012) 683–701, http://dx.doi.org/10.3390/en5030683.
[13] S. Pindado, J. Pérez, S. Avila-Sanchez, On cup anemometer rotor aerodynamics, Sensors 12 (2012) 6198–6217, http://dx.doi.org/10.3390/s120506198.
[14] S. Pindado, I. Pérez, M. Aguado, Fourier analysis of the aerodynamic behavior of cup anemometers, Meas. Sci. Technol. 24 (2013) 065802, http://dx.doi.org/10.1088/0957-0233/24/6/065802 (9 pp).
[15] S. Pindado, J. Cubas, A. Sanz-Andrés, Aerodynamic analysis of cup anemometers performance. The stationary harmonic response, Sci. World J. 2013 (2013) 1–11, http://dx.doi.org/10.1155/2013/197325.
[16] A. Sanz-Andrés, S. Pindado, F. Sorribes, Mathematical analysis of the effect of the rotor geometry on cup anemometer response, Sci. World J. 2014 (2014) 1–23, http://dx.doi.org/10.1155/2014/537813.
[17] M.C.-E. Brazier, Sur la variation des indications des anémomètres Robinson et Richard en fonction de l'inclinaison du vent, Comptes Rendus Des Séances l'Académie Des Sci. 170 (1920) 610–612.
[18] L. Kristensen, The cup anemometer and other exciting instruments. Risø–R–615 (EN), Roskilde, Denmark, 1993.
[19] International Electrotechnical Commission, International Standard IEC-61400-12-1. Wind Turbines. Part 12-1: Power performance measurements of electricity producing wind turbines, first ed., 2005-12, 2005.
[20] MEASNET, Anemometer calibration procedure, Version 2 (October 2009), Madrid, Spain, 2009.
[21] MEASNET, Cup anemometer calibration procedure, Version 1 (September 1997, updated 24/11/2008), Madrid, Spain, 1997.
[22] ASTM International, Standard Test Method for Determining the Performance of a Cup Anemometer or Propeller Anemometer (ASTM D 5096-02), ASTM International, West Conshohocken, PA 19428, USA, 2002.

[23] S. Ramachandran, A theoretical study of cup and vane anemometers, Q. J. R. Meteorol. Soc. 95 (1969) 163–180.
[24] J. Kondo, G.I. Naito, Y. Fujinawa, Response of Cup Anemometer in Turbulence, J. Meteorol. Soc. Jpn. 49 (1971) 63–74.
[25] T.F. Pedersen, Development of a Classification System for Cup Anemometers – CLASSCUP. Risø-R-1348(EN), Roskilde, Denmark, 2003.
[26] E.I. Kaganov, A.M. Yaglom, Errors in wind-speed measurements by rotation anemometers, Boundary-Layer Meteorol. 10 (1976) 15–34.
[27] Y.P. Solov'ev, A.I. Korovushkin, Y.N. Toloknov, Characteristics of a cup anemometer and a procedure of measuring the wind velocity, Phys. Oceanogr. 14 (2004) 173–186.
[28] M.J. Brevoort, U.T. Joyner, Experimental investigation of the Robinson-type cup anemometer. NACA TN-513, 1935.
[29] O. Schrenk, Über die Trägheitsfehler des Schalenkreuz-Anemometers bei schwankender Windstärke, Zeitschrift Fur Tech. Phys. 10 (1929) 57–66.
[30] J.C. Wyngaard, Cup, propeller, vane, and sonic anemometers in turbulence research, Annu. Rev. Fluid Mech. 13 (1981) 399–423.
[31] J. Patterson, The cup anemometer, Trans. R. Soc. Canada Ser. III 20 (1926) 1–54.
[32] E. Vega, S. Pindado, A. Martínez, E. Meseguer, L. García, Anomaly detection on cup anemometers, Meas. Sci. Technol. 25 (2014) 127002 (6pp).
[33] N. Stefanatos, P. Papadopoulos, E. Binopoulos, A. Kostakos, G. Spyridakis, Effects of long term operation on the performance characteristics of cup anemometers, in: Eur. Wind Energy Conf. Exhib. EWEC 2007, 7–10 May, Milan, Italy, 2007, pp. 1–6.
[34] K.H. Papadopoulos, N.C. Stefanatos, U.S. Paulsen, E. Morfiadakis, Effects of turbulence and flow inclination on the performance of cup anemometers in the field, Boundary-Layer Meteorol. 101 (2001) 77–107.
[35] L. Kristensen, G. Jensen, A. Hansen, P. Kirkegaard, Field Calibration of Cup Anemometers. Risø–R–1218(EN), Roskilde, Denmark, 2001.
[36] U.S. Paulsen, N.G. Mortensen, J.C. Hansen, U.S. Said, A.S. Mousa, Field calibration of cup anemometers, in: Eur. Wind Energy Conf. Exhib. EWEC 2007, 7–10 May, Milan, Italy, 2007, pp. 1–8.
[37] D. Laguigne, B. Roni-Damon, EP 2 037 284 B1 Patent. Procédé et dispositif pour vérifier le bon fonctionnement d'un anémomètre (Method and device to check the correct operation of an anemometer), EP 2 037 284 B1, 2010.
[38] H. Ema, H. Funio, W. Masato, T. Yasuhide, K. Hitoshi, T. Yasuo, et al., JP 10227810 A Patent. Testing apparatus and method for anemometer, JP 10227810 A, 1998.
[39] J.S. Frost, D.A. Haines, R.J. Klumpp, US 4365504 A Patent. Method and apparatus for field testing of anemometers, 1982.
[40] D.S. Cummings, US 20110283766 A1 Patent. Apparatus and Calibration Method for Cup Anemometers having Non-Removable Cupsets, 2011.
[41] G.P. Corten, WO 2001035109 A1 Patent. Method for testing an anemometer, WO 2001035109 A1, 2001.
[42] T. Siebers, H.-J. Kooijman, D. Rogers, US 20080307853 A1 Patent. Anemometer calibration method and wind turbine, 2008.
[43] A. Wobben, EP 1454058 A1 Patent. Method for monitoring a sensor, EP 1454058 A1, 2010.
[44] J. Beltrán, A. Llombart, J. Guerrero, A bin method with data range selection for detection of nacelle anemometers faults, in: Eur. Wind Energy Conf. Exhib. EWEC 2009, 17–19 March, Marseille, France, 2009, pp. 1–8. <http://teide.cps.unizar.es:8080/pub/publicir.nsf/codigospub/0562/$FILE/cp0562.pdf> (accessed 02.12.13).
[45] J. Beltrán, A. Llombart, J. Guerrero, Detection of nacelle anemometers faults in a wind farm, in: Proc. Int. Conf. Renew. Energies Power Qual. ICREPQ 2009, 15–17 April, Valencia, Spain, 2009, pp. 1–6. <http://teide.cps.unizar.es:8080/pub/publicir.nsf/codigospub/0561/$FILE/cp0561.pdf> (accessed 02.12.13).
[46] M.J. Desforges, P.J. Jacob, J.E. Cooper, Applications of probability density estimation to the detection of abnormal conditions in engineering, Proc. Inst. Mech. Eng. Part C: J. Mech. Eng. Sci. 212 (1998) 687–703, http://dx.doi.org/10.1243/0954406981521448.
[47] B. Lu, Y. Li, X. Wu, Z. Yang, A review of recent advances in wind turbine condition monitoring and fault diagnosis, in: Power Electron. Mach. Wind Appl. 2009. PEMWA 2009. IEEE, 2009. <http://ieeexplore.ieee.org/xpls/abs_all.jsp?arnumber=5208325> (accessed 23.12.13).
[48] F.P. García Márquez, A.M. Tobias, J.M. Pinar Pérez, M. Papaelias, Condition monitoring of wind turbines: techniques and methods, Renew. Energy 46 (2012) 169–178, http://dx.doi.org/10.1016/j.renene.2012.03.003.
[49] Z. Hameed, Y.S. Hong, Y.M. Cho, S.H. Ahn, C.K. Song, Condition monitoring and fault detection of wind turbines and related algorithms: a review, Renew. Sustain. Energy Rev. 13 (2009) 1–39, http://dx.doi.org/10.1016/j.rser.2007.05.008.
[50] C. Hatch, Condition monitoring using acceleration enveloping, Orbit 61 (2004) 58–61.
[51] V. Chandola, A. Banerjee, V. Kumar, Anomaly detection, ACM Comput. Surv. 41 (2009) 1–58, http://dx.doi.org/10.1145/1541880.1541882.
[52] E. Keogh, K. Chakrabarti, M. Pazzani, S. Mehrotra, Dimensionality reduction for fast similarity search in large time series databases, Knowl. Inf. Syst. 3 (2001) 263–286. <http://link.springer.com/article/10.1007/PL00011669> (accessed 12.02.14).
[53] Y. Dong, Z. Sun, H. Jia, A cosine similarity-based negative selection algorithm for time series novelty detection, Mech. Syst. Signal Process. 20 (2006) 1461–1472, http://dx.doi.org/10.1016/j.ymssp.2004.12.006.
[54] E. Keogh, J. Lin, S.-H. Lee, H. Van Herle, Finding the most unusual time series subsequence: algorithms and applications, Knowl. Inf. Syst. 11 (2006) 1–27, http://dx.doi.org/10.1007/s10115-006-0034-6.
[55] L. Sun, C. Chen, Q. Cheng, Feature extraction and pattern identification for anemometer condition diagnosis, Int. J. Prognost. Heal. Manage. 3 (2012) 8–18.
[56] J. Cassity, C. Aven, D. Parker, Applying Weibull distribution and discriminant function techniques to predict damaged cup, anemometers in the 2011 PHM competition, Int. J. Prognost. Heal. Manage. 3 (2012) 1–7.
[57] D. Siegel, J. Lee, An auto-associative residual processing and K-means clustering approach for anemometer health assessment, Int. J. Prognost. Heal. Manage. 2 (2011) 50–61.
[58] A. Bégin-Drolet, J. Lemay, J. Ruel, Time domain modeling of cup anemometers using artificial neural networks, Flow Meas. Instrum. 33 (2013) 10–27, http://dx.doi.org/10.1016/j.flowmeasinst.2013.04.012.
[59] T.F. Pedersen, U.S. Paulsen, Classification of operational characteristics of commercial cup-anemometers, in: EWEC-CONFERENCE 1999, Nice, France, 1999, pp. 611–615.
[60] T.F. Pedersen, Characterisation and Classification of RISØ P2546 Cup Anemometer. Risø-R-1364(EN), second ed., Roskilde, Denmark, 2004.
[61] T.F. Pedersen, J.-Å. Dahlberg, P. Busche, ACCUWIND -Classification of Five Cup Anemometers According to IEC61400-12-1. Risø-R-1556(EN), Roskilde, Denmark, 2006.
[62] S. Pindado, J. Cubas, F. Sorribes-Palmer, The cup anemometer, a fundamental meteorological instrument for the wind energy industry. Research at the IDR/UPM Institute, Sensors 14 (2014) 21418–21452, http://dx.doi.org/10.3390/s141121418.
[63] ENAC, Anexo Técnico. Acreditación Nº 134/LC10. 095. INSTITUTO UNIVERSITARIO DE MICROGRAVEDAD "IGNACIO DA RIVA", 2012. <https://www.enac.es/documents/7020/67cfa73f-f539-4c13-8172-986daad8514a> (accessed 29.01.14).
[64] J.-Å. Dahlberg, T.F. Pedersen, P. Busche, ACCUWIND -Methods for Classification of Cup Anemometers. Risø-R-1555(EN), Roskilde, Denmark, 2006.
[65] D. Lindley, The design and performance of a 6-cup anemometer, J. Appl. Meteorol. 14 (1975) 1135–1145.
[66] T.R. Robinson, On a new anemometer, Proc. R. Irish Acad. (1836–1869) 4 (1847) 566–572.
[67] T.R. Robinson, On the determination of the constants of the cup anemometer by experiments with a whirling machine. Part II, Philos. Trans. R. Soc. Lond. 171 (1880) 1055–1070, http://dx.doi.org/10.1098/rstl.1880.0025.
[68] T.R. Robinson, On the determination of the constants of the cup anemometer by experiments with a whirling machine, Philos. Trans. R. Soc. Lond. 169 (1878) 777–822.
[69] P.A. Sheppard, Anemometry: a critical and historical survey, Proc. Phys. Soc. 53 (1941) 361–390.
[70] A.F. Spilhaus, C. Rossby, Analysis of the Cup Anemometer (Meteorological Course. Professional Notes – No. 7), Cambridge, Massachusetts, USA, 1934. <http://scholar.google.com/scholar?hl=en&btnG=Search&q=intitle:Analysis+of+the+cup+anemometer#1> (accessed 27.08.13).
[71] S.P. Fergusson, Harvard Meteorological Studies No. 4. Experimental Studies of Cup Anemometers, Harvard University Press, Cambridge, Massachusetts, USA, 1939.